

Design, Synthesis, and Evaluation of Orally Active 4-(2,4-Difluoro-5-(methoxycarbamoyl)phenylamino)pyrrolo[2,1-f][1,2,4]triazines as Dual Vascular Endothelial Growth Factor Receptor-2 and Fibroblast Growth Factor Receptor-1 Inhibitors

Robert M. Borzilleri,^{*,†} Xiaoping Zheng,[†] Ligang Qian,[†] Christopher Ellis,[†] Zhen-wei Cai,[†] Barri S. Wautlet,[‡] Steve Mortillo,[‡] Robert Jeyaseelan, Sr.,[‡] Daniel W. Kukral,[‡] Aberra Fura,[§] Amrita Kamath,[§] Viral Vyas,[§] John S. Tokarski,^{||} Joel C. Barrish,[†] John T. Hunt,[‡] Louis J. Lombardo,[†] Joseph Fargnoli,[‡] and Rajeev S. Bhide[†]

Departments of Oncology Chemistry, Discovery Biology, Metabolism and Pharmacokinetics, and Structural Biology and Modeling, Bristol-Myers Squibb Pharmaceutical Research Institute, P.O. Box 4000, Princeton, New Jersey 08543-4000

Received February 9, 2005

A series of substituted 4-(2,4-difluoro-5-(methoxycarbamoyl)phenylamino)pyrrolo[2,1-f][1,2,4]-triazines was identified as potent and selective inhibitors of the tyrosine kinase activity of the growth factor receptors VEGFR-2 (Flk-1, KDR) and FGFR-1. The enzyme kinetics associated with the VEGFR-2 inhibition of compound **50** ($K_i = 52 \pm 3$ nM) confirmed that the pyrrolo[2,1-f][1,2,4]triazine analogues are competitive with ATP. Several analogues demonstrated low-nanomolar inhibition of VEGF- and FGF-dependent human umbilical vein endothelial cell (HUVEC) proliferation. Replacement of the C6-ester substituent of the pyrrolo[2,1-f][1,2,4]-triazine core with heterocyclic bioisosteres, such as substituted 1,3,5-oxadiazoles, afforded compounds with excellent oral bioavailability in mice (i.e., **50** $F_{po} = 79\%$). Significant antitumor efficacy was observed with compounds **44**, **49**, and **50** against established L2987 human lung carcinoma xenografts implanted in athymic mice. A full account of the synthesis, structure–activity relationships, pharmacology, and pharmacokinetic properties of analogues within the series is presented.

Introduction

Angiogenesis is an essential series of molecular events that occurs during the formation of new blood vessels from the endothelium of preexisting vasculature.¹ This tightly regulated process is dependent on a delicate balance between pro- and antiangiogenic factors,² and serves as an integral component for physiological processes, such as embryonic development, female reproductive function, and wound healing. Uncontrollable or pathological angiogenesis, however, has been implicated in a wide array of vascular hyperproliferative disorders, most notably cancer, rheumatoid arthritis, diabetic retinopathy, age-related macular degeneration, and psoriasis.^{3–4} It is well established that an efficient blood supply is required for solid tumors to sustain growth beyond a critical size and to metastasize to other organs. Tumor-induced angiogenesis is responsible for the newly formed capillary networks between host and tumor that allow for effective delivery of oxygen and essential nutrients to cancer cells, elimination of waste materials generated from tumor metabolism, and migration of cancer cells to remote sites leading to metastasis.⁵

Tumor cells respond to a variety of stimuli, such as hypoxia, low pH, changes in interstitial fluid pressure, growth factors, or cytokines by up-regulating the expression of proangiogenic factors. Vascular endothelial growth factor (VEGF; vascular permeability factor,

VPF),⁶ a key stimulator of tumor angiogenesis, promotes endothelial cell proliferation, survival, migration, invasion, and differentiation. The intrinsic activity responsible for these cellular events is dependent on the highly specific binding of the VEGF ligands (isoforms) to their respective cell surface expressed receptors VEGFR-1 (Flt-1), VEGFR-2 (KDR, Flk-1), and VEGFR-3 (Flt-4). Activation of the VEGF receptor tyrosine kinases (RTKs), which are highly expressed on vascular endothelial cells, leads to receptor dimerization, autophosphorylation of key tyrosine residues within the catalytic domain, and the initiation of downstream signaling cascades that regulate tumor progression and dissemination.

Throughout the past decade, RTKs have received considerable attention as attractive molecular targets for drug discovery.^{7,8} Monoclonal antibodies specific for kinase ligands or their receptors, and small molecule inhibitors that interact at the ATP-binding site of a given kinase domain have demonstrated promising therapeutic utility.⁹ For example, the chimeric anti-VEGF monoclonal antibody bevacizumab (Genentech) recently afforded a significant survival benefit in metastatic colorectal cancer patients when combined with standard chemotherapy (IFL or Saltz regimen).¹⁰ These key clinical findings provided the proof-of-concept for therapies aimed at controlling abnormal vascular development operative in cancer progression. Orally active, small molecule inhibitors of VEGFR-2 kinase activity from several structural classes¹¹ (i.e., phthalazines,¹² indolinones,¹³ quinazolines,¹⁴ isothiazoles,^{15a} thienopyridines,^{15b} indeno[2,1- α]pyrrolo[3,4-c]carbazolones,¹⁶ thiazoles,^{17a} pyridines,^{17b} indoles,^{17c,d} imidazopyri-

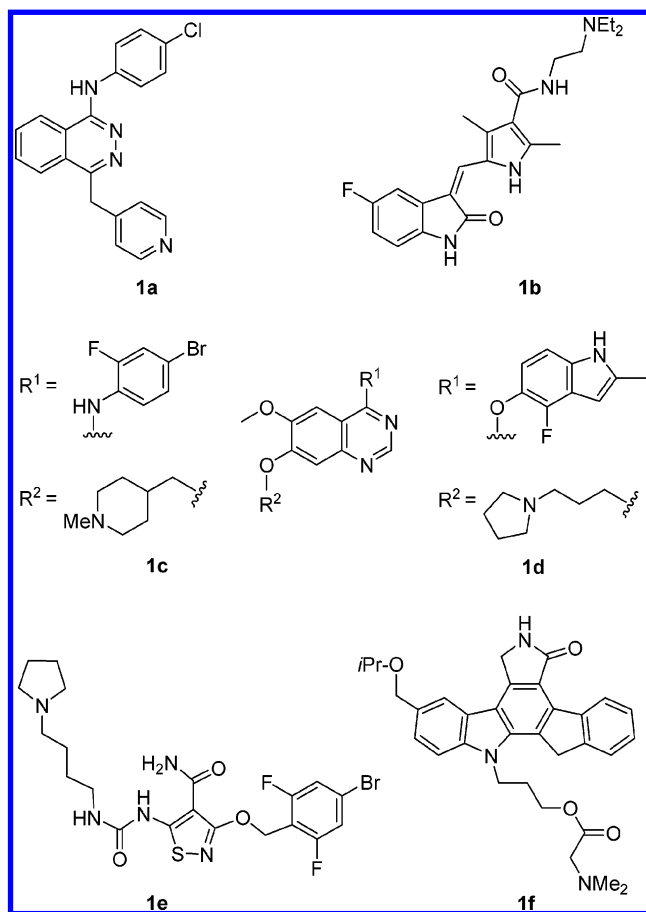
* To whom correspondence should be addressed. Phone: (609) 252-6236. Fax: (609) 252-7410. E-mail: robert.borzilleri@bms.com.

[†] Department of Oncology Chemistry.

[‡] Department of Discovery Biology.

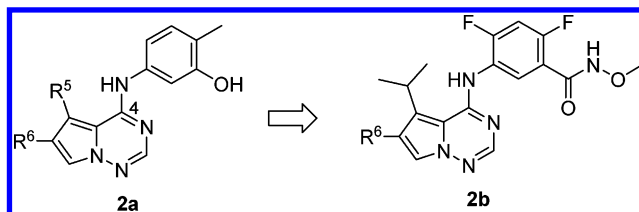
[§] Department of Metabolism and Pharmacokinetics.

^{||} Department of Structural Biology and Modeling.

Chart 1. Examples of VEGFR-2 Inhibitors Undergoing Clinical Trials

dines,^{17e} benzimidazoles,^{17f} pyrimidines,^{17g-i} diamino-[1,3,5]triazines,^{18a} biheteroaryls^{18b}) have also progressed to various stages of preclinical and clinical development. Representative examples of VEGFR-2 inhibitors currently undergoing clinical evaluation are illustrated in Chart 1. Novartis' anilino-phthalazine PTK-787 (vatalanib, **1a**)^{12a,b} and Pfizer's (Sugen/Pharmacia) third-generation indolinone SU-11248 (**1b**)^{13a,b} are the most advanced agents, currently in phase III clinical trials. AstraZeneca and Pfizer have initiated phase II clinical trials for quinazoline ZD-6474 (vandetanib, **1c**)^{14a,b} and isothiazole CP-547632 (**1e**),^{15a} respectively. The indeno-pyrrolo-carbazole *N,N*-dimethylglycine ester prodrug CEP-7055¹⁶ (**1f**, Cephalon) and a second-generation quinazoline AZD-2171 (**1d**, AstraZeneca) have also entered the clinic. Each of these structurally diverse chemotypes offer distinct kinase selectivity profiles relative to VEGFR-2 activity that may ultimately influence their overall therapeutic potential.

Fibroblast growth factor (FGF) represents another important family of angiogenic growth factors.¹⁹ While the exact role of FGF in tumor angiogenesis remains elusive, this potent mitogen of vascular endothelial cells and fibroblasts is believed to cooperate with VEGF during blood vessel development.²⁰ Since VEGFR-2 and FGFR-1 have been shown to directly influence tumor angiogenesis, simultaneous inhibition of these two RTKs is postulated to enhance antitumor activity. To this end, small molecule inhibitors of FGFR-1,²¹ including indolinone derivatives^{13c} that inhibit VEGFR-2, FGFR-1, and PDGFR- β have appeared in the literature. Furthermore,

**Figure 1.** Evolution of the hydroxamate series of VEGFR-2 inhibitors.

since antiangiogenic therapies are directed toward highly regulated endothelial cells of the host, rather than genetically unstable tumor cells, it is anticipated that selective VEGFR-2 and/or FGFR-1 inhibition will lead to cancer therapeutics that have a lower risk of developing classical drug resistance compared to traditional chemotherapy.²²

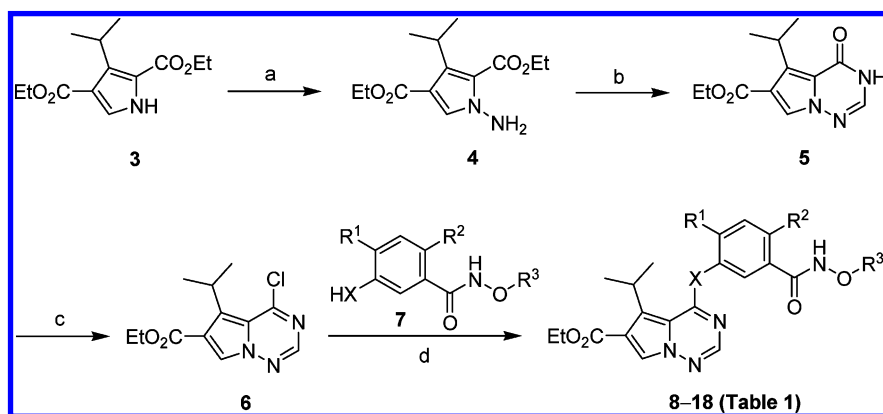
As part of our continuing effort to identify selective small molecule RTK inhibitors for various oncology indications, we have identified the pyrrolo[2,1-*f*][1,2,4]-triazine nucleus as a general kinase inhibitor template.²³ In our search for selective VEGFR-2 kinase inhibitors, we have recently disclosed the structure-activity relationships (SARs) of 4-(3-hydroxy-4-methylphenylamino)pyrrolo[2,1-*f*][1,2,4]triazines **2a** (Figure 1).^{24a} Herein, we describe the SAR, pharmacokinetics, and pharmacology of the novel series of 4-(2,4-difluoro-5-(methoxycarbonyl)phenylamino)pyrrolo[2,1-*f*][1,2,4]-triazines **2b** that were derived from the phenol analogues and a structurally related series of p38 MAP kinase inhibitors.^{24b} These studies culminated in the identification of potent, orally active dual inhibitors of VEGFR-2 and FGFR-1 from the hydroxamate series that demonstrated robust antitumor activity in the L2987 human lung carcinoma xenograft model.

Chemistry

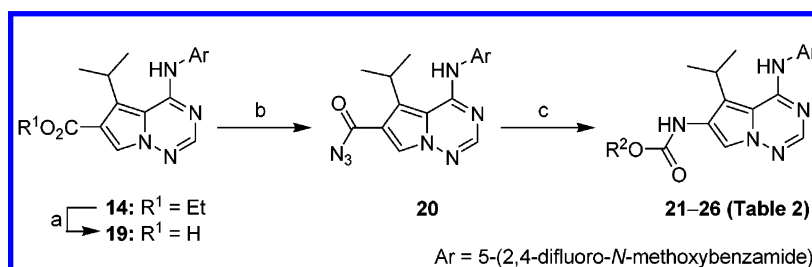
Pyrrolo[2,1-*f*][1,2,4]triazine derivatives **8–18** were prepared according to the general synthetic sequence outlined in Scheme 1. The pyrrolo-triazinone core **5** was assembled using a modified version of the literature procedure of Patil et al.²⁵ *N*-Amination of diethyl 3-isopropyl-1*H*-pyrrole-2,4-dicarboxylate (**3**)²⁶ using either *O*-(diphenylphosphinyl)hydroxylamine or *O*-(mesitylenesulfonyl)hydroxylamine provided aminopyrrole **4**. Cyclization of **4** upon heating in formamide generated the desired bicycle **5**. Treatment of intermediate **5** with phosphorus oxychloride afforded chloroimidate **6**, which was subsequently coupled with the appropriately functionalized 3-hydroxy or 3-amino-*N*-alkoxybenzamides **7** to furnish the corresponding analogues **8–18** in good overall yield.

A small library of C6-carbamate analogues (cf. Supporting Information) was prepared from the stable acyl azide intermediate **20** using a parallel, solution phase format (Scheme 2). Thus, carboxylic acid **19**, derived from base-promoted hydrolysis of ethyl ester **14**, was treated with diphenylphosphoryl azide (DPPA) in the presence of triethylamine to furnish compound **20**. Curtius rearrangement of the acyl azide **20**, in the presence of commercially available alcohols, produced the desired carbamate derivatives, including examples **21–26**.

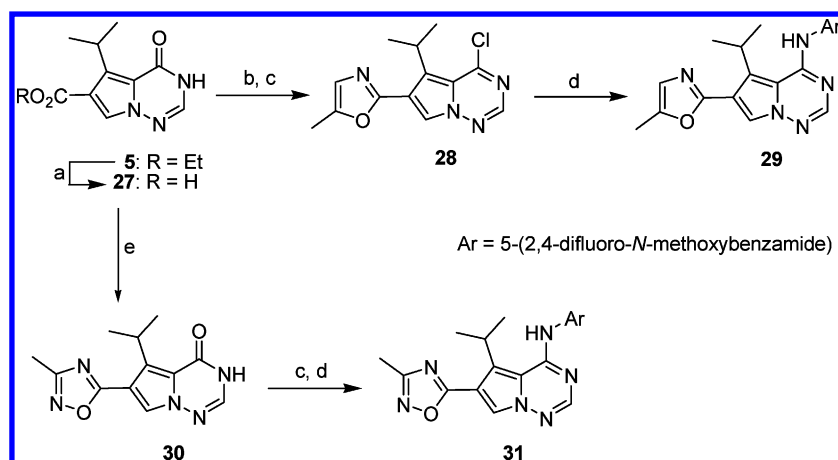
Five-membered ring heterocycles were installed at the 6-position of the pyrrolo[2,1-*f*][1,2,4]triazine nucleus

Scheme 1^a

^a Reagents and conditions: (a) $\text{Ph}_2\text{PO}_2\text{NH}_2$ or $\text{Me}_3\text{PhSO}_3\text{NH}_2$, NaH, DMF, 85%; (b) formamide, 165 °C, 90%; (c) POCl_3 , 110 °C, 3 h, 90%; (d) X = O: K_2CO_3 , DMF, 25 °C, 18 h, X = NH: DMF, 25 °C, 12–18 h.

Scheme 2^a

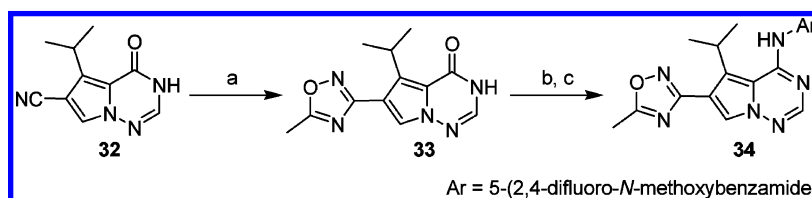
^a Reagents and conditions: (a) 1 N NaOH, THF– H_2O , 60 °C, 27 h, 98%; (b) DPPA, 1,4-dioxane, Et_3N , 40 °C, 1 h, 99%; (c) R^2OH , DMF, 85 °C, 2 h, 50–65%.

Scheme 3^a

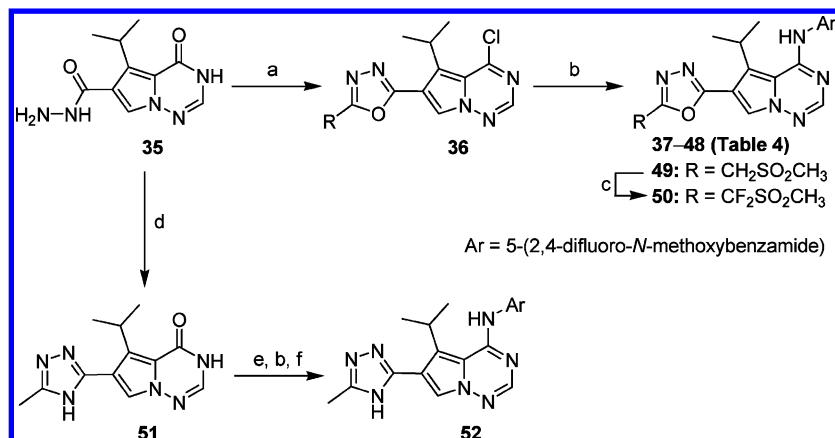
^a Reagents and conditions: (a) 1 N NaOH, THF– H_2O , 60 °C, 98%; (b) 1-aminopropan-2-one, BOP reagent, Et_3N , DMF, 50 °C, 2 h, 61%; (c) POCl_3 , 120 °C, 6 h; (d) 5-amino-2,4-difluoro-*N*-methoxybenzamide, MeCN, 25 °C, 18 h; (e) (1) *N*-hydroxyacetamide, TBTU, cat. HOBt, *i*- Pr_2NEt , DMF, 1.5 h, (2) DMF, 140 °C, 3 h, 57% overall.

according to the synthetic sequences illustrated in Schemes 3–5.^{27–32} As shown in Scheme 3, the pyrrolo-triazinone ester **5** was hydrolyzed under mild heating to provide carboxylic acid **27**. Oxazole **28** and 1,2,4-oxadiazole **30** were prepared from intermediate **27** by two independent routes. Standard amide bond coupling of compound **27** with 1-aminopropan-2-one was accomplished with benzotriazol-1-yloxy-tris(dimethylamino)phosphonium hexafluorophosphate (BOP). The amide intermediate was heated with phosphorus oxychloride to promote simultaneous cyclization and chloroimidate formation to furnish **28**. Alternatively, acid **27** was coupled to *N*-hydroxyacetamide in the presence of *O*-(1*H*-benzotriazol-1-yl)-*N,N,N',N'*-tetramethyluronium

tetrafluoroborate (TBTU) and then cyclized under thermal conditions to generate **30** in good overall yield. Treatment of compound **28** and the chloroimidate derived from pyrrolo-triazinone **30** with 5-amino-2,4-difluoro-*N*-methoxybenzamide provided the fully elaborated analogues **29** and **31**, respectively. The regioisomeric 1,2,4-oxadiazole **34** was prepared from the chloroimidate obtained from pyrrolo-triazinone **33** using similar chemistry (Scheme 4). The nitrile **32**, derived from carboxylic acid **27**, was converted to the 1,2,4-oxadiazole **33** using an unoptimized, two-step procedure involving the cyclization of the requisite *N*-hydroxyacetamide intermediate with acetyl chloride in refluxing pyridine.

Scheme 4^a

^a Reagents and conditions: (a) (1) $\text{NH}_2\text{OH}\cdot\text{HCl}$, K_2CO_3 , EtOH reflux, 28 h, (2) AcCl , pyridine reflux, 7 h, 11% overall; (b) POCl_3 , 120 °C, 5 h; (c) 5-amino-2,4-difluoro-*N*-methoxybenzamide, MeCN, 25 °C, 14 h; 30% from **33**.

Scheme 5^a

^a Reagents and conditions: (a) RCO_2H , POCl_3 , 100 °C, 1 h then 120 °C, 3 h; (b) 5-amino-2,4-difluoro-*N*-methoxybenzamide, DMF, 50 °C, 1–6 h; (c) $\text{LiN}[\text{Si}(\text{CH}_3)_3]_2$, $(\text{PhSO}_2)_2\text{NF}$, THF, –78 to –30 °C, 1 h, 65%; (d) acetamide- HCl , DMF, 120 °C, 1 h, 86%; (e) POCl_3 , 120 °C, 5 h; (f) 71% overall yield from **51**.

The hydrazide intermediate **35**, obtained from the reaction of ester **5** with hydrazine, was used to prepare 1,3,4-oxadiazoles **37–49** and triazole **52** (Scheme 5). The C6-heterocycles of compounds **36** and **51** were installed under thermal conditions, using either the corresponding carboxylic acid in phosphorus oxychloride or acetamide hydrochloride in DMF. Alternatively, the oxadiazole rings of compounds **38** and **47** were prepared from hydrazide **35** using triethyl orthoformate³⁰ and phosgene imminium chloride,³³ respectively (cf. Experimental Section). Chemistry described previously was used to convert compounds **36** and **51** to the desired VEGFR-2 inhibitors **37–49** and **52**, respectively. Difluorination of compound **49** was carried out at low temperature in THF using excess lithium bis(trimethylsilyl)amide and 2.5 equiv of commercially available *N*-fluorobenzenesulfonimide to furnish the desired oxadiazole analogue **50** in 65% yield.

Results and Discussion

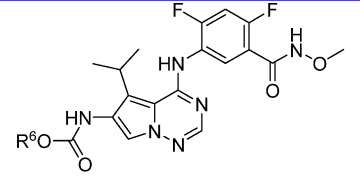
In Vitro Pharmacology and SAR. The pyrrolo[2,1-*f*][1,2,4]triazine analogues depicted in Tables 1–4 were initially screened and optimized for inhibition of human VEGFR-2 tyrosine kinase activity. Potent analogues ($\text{IC}_{50} < 100$ nM) identified in the primary biochemical assay²³ were then evaluated for inhibition of FGFR-1 kinase activity. Select compounds were subsequently screened for enzyme inhibition against a small panel of RTKs [Flk-1, PDGFR- β , HER-1 (EGFR), HER-2, IGF-1R] utilizing a previously reported assay format.²³ In each case, the entire cytoplasmic domain sequence of the RTK was fused to glutathione *S*-transferase and the biological activity was determined by quantitation of the amount of radioactive phosphate transferred to an artificial poly(Glu₄/Tyr) substrate. Procedures for mea-

Table 1. Effect of the C4-Substituent on Enzymatic Activity^a

compd	X	R ¹	R ²	R ³	IC ₅₀ (nM) for VEGFR-2 kinase inhibn ^b
8	O	H	H	Me	270
9	NH	H	H	Me	130
10	NH	H	Me	Me	120
11	NH	H	Br	Me	270
12	NH	H	F	Me	79
13	NH	F	H	Me	34
14	NH	F	F	Me	13
15	NH	F	F	Et	40
16	NH	F	F	<i>i</i> -Pr	350
17	NH	F	F	<i>i</i> -Bu	1200
18	NH	F	F	CH ₂ -cyc ^c	190

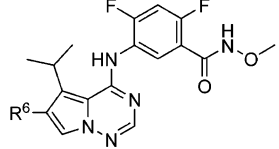
^a See Experimental Section for a description of the assay conditions. ^b IC₅₀ values are reported as the mean of at least three determinations. Variability around the mean value was <25%. ^c cyc = cyclopropyl.

suring activity against the representative nonreceptor kinase LCK and the serine-threonine kinases PKC α and CDK2 have also been described previously.^{34,35} The most potent and selective VEGFR-2 and FGFR-1 inhibitors were evaluated for their ability to inhibit growth-factor-stimulated cellular proliferation of human umbilical vein endothelial cells (HUVECs) using either VEGF or FGF as the mitogen.²³ As a positive control for general cytotoxicity, compounds evaluated in the HUVEC assays were also tested for their ability to inhibit the proliferation of the L2987 human lung carcinoma cell line. In all cases, the pyrrolotriazine analogues described

Table 2. Effect of C6-Carbamates on Enzymatic and Cellular Activity^a


compd	R ⁶	IC ₅₀ (nM)	
		VEGFR-2 kinase inhibition ^b	growth inhibition of HUVECs ^c driven by VEGF
21	Et	66	31
22	Bn	180	ND ^d
23	-(CH ₂) ₃ -piperidine	79	62
24	-(CH ₂) ₃ SO ₂ Me	62	100
25		58	46
26		36	19

^a See Experimental Section for a description of the assay conditions. ^b IC₅₀ values are reported as the mean of at least three determinations. Variability around the mean value was <25%. ^c Human umbilical vein endothelial cells. ^d ND = not determined.

Table 3. Comparison of VEGFR-2 and FGFR-1 Biochemical and Cellular Potencies^a for C6-Heterocyclic Analogues


compd	R ⁶	IC ₅₀ (nM)			
		kinase inhibition ^b		growth inhibition of HUVECs ^c stimulated by:	
		VEGFR-2	FGFR-1	VEGF	FGF
29		8.0	20	1.1	4.0
31		49	110	6.8	7.6
34		110	140	ND ^d	ND
37		18	19	7.6	6.5
52		71	50	50	46

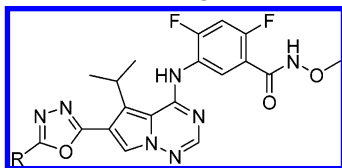
^a See Experimental Section for a description of the assay conditions. ^b IC₅₀ values are reported as the mean of at least three determinations. Variability around the mean value was <50%. ^c Human umbilical vein endothelial cells. ^d ND = not determined.

herein provided IC₅₀ values >1.3 μM in the unstimulated growth of L2987 cells.

The pyrrolo[2,1-*f*][1,2,4]triazine nucleus with the C5-isopropyl and C6-ethyl ester substituents served as the starting template for the hydroxamate series of VEGFR-2 kinase inhibitors based on our previous SAR investigations involving the 4-(3-hydroxy-4-methylphenylamino)pyrrolo[2,1-*f*][1,2,4]triazines.²⁴ Table 1 sum-

marizes the SAR of the C4-hydroxamate group with respect to inhibition of VEGFR-2 kinase activity. Consistent with our earlier observations in the phenol series,²⁴ the amine linker (X = NH) provided compounds that were slightly more potent against VEGFR-2 kinase than the corresponding ether analogues (i.e., **9** versus **8**). *N*-Methylation of the hydroxamate group of compound **9** provided ethyl 5-isopropyl-4-(3-(methoxymethyl)carbamoyl)phenylamino)pyrrolo[2,1-*f*][1,2,4]triazine-6-carboxylate (structure not shown), which was >30-fold less potent in the biochemical assay. The significant reduction in activity supports the hypothesis that the hydroxamate-NH participates in hydrogen-bonding interactions within the VEGFR-2 kinase domain (vide infra). Addition of a methyl substituent at R² (i.e., **10**) had minimal effect on the intrinsic activity, while the bromide analogue **11** (R² = Br) was >2-fold less potent than the parent hydroxamate derivative **9**. Incorporation of a fluorine atom at R² was well-tolerated, although the fluorine atom of analogue **13** (R¹ = F) had a greater impact on the VEGFR-2 kinase activity compared to compound **12**. The 2,4-difluoro analogue **14** was one order of magnitude more potent than the original lead **9** in the kinase assay and displayed excellent cellular potency (IC₅₀ = 4.8 nM) in the VEGF-driven HUVEC proliferation assay. Increasing the size of hydroxamate substituent R³ (i.e., **15**–**18**) was detrimental to the kinase activity. Since an electron-deficient phenyl ring provides a significant enhancement in the VEGFR-2 kinase inhibition, the 2,4-difluoro-5-(methoxycarbonyl)phenylamino group was selected as the preferred C4-substituent for subsequent SAR studies.

The C6-carbamate analogues obtained from the library synthesis were initially screened for VEGFR-2 kinase inhibition at concentrations of 0.2 and 0.05 μM (cf. Supporting Information). The IC₅₀ values were then determined for select compounds of interest, which provided ≥50% inhibition at 0.05 μM in the preliminary two-point assay. Table 2 highlights representative carbamate analogues from the library that offer different physicochemical properties and a range of in vitro rates of metabolism in human liver microsomes (vide infra). In contrast to the SAR observed with the phenol series,²⁴ replacement of the metabolically labile C6-ester moiety³⁶ of compound **14** with a carbamate group provided pyrrolo[2,1-*f*][1,2,4]triazine analogues that were consistently less potent against VEGFR-2 kinase. For example, carbamates **21** and **22** were 5- and 14-fold less potent than ester analogue **14**, respectively. On the basis of the proposed binding mode of the pyrrolo[2,1-*f*][1,2,4]triazines in the VEGFR-2 kinase domain, the C6-substituents extend out toward the protein surface and potentially interact with solvent. Thus, appending a terminal piperidine or methyl sulfone substituent to the carbamate via a 3-carbon linker was found to be well-tolerated (i.e., **23** and **24**). Tetrahydrofuran analogue **25** provided comparable enzymatic activity to compound **21**, whereas the *N*-methylpiperazine derivative **26** was the most potent carbamate analogue in both the kinase and cellular proliferation assays, providing IC₅₀ values of 36 and 19 nM, respectively. As shown in Table 2, in most cases there is good agreement between the IC₅₀ values obtained in the VEGFR-2 kinase and VEGF-stimulated HUVEC proliferation assays for the carbamate series.

Table 4. VEGFR-2 and FGFR-1 Biochemical and Cellular Potencies^a of C6-Oxadiazole Analogues

compd	R	IC ₅₀ (nM)			
		kinase inhibition ^b		growth inhibition of HUVECs ^c	
		VEGFR-2	FGFR-1	VEGF	FGF
38	H	77	160	91	54
39	Et	17	28	1.8	4.7
40	<i>i</i> -Pr	22	39	18	1.0
41	<i>i</i> -Bu	23	33	2.1	6.6
42	cyclopropyl	11	14	3.6	5.3
43	CH ₂ -cyclopropyl	17	27	4.0	9.2
44	CHF ₂	57	100	17	21
45	CF ₃	76	84	35	33
46	CH ₂ CF ₃	29	68	25	44
47	N(CH ₃) ₂	11	18	6.7	7.3
48	CH ₂ N(CH ₃) ₂	66	149	ND ^d	ND
49	CH ₂ SO ₂ CH ₃	16	16	2.1	4.6
50	CF ₂ SO ₂ CH ₃	53	220	27	130

^a See Experimental Section for a description of the assay conditions. ^b IC₅₀ values are reported as the mean of at least three determinations. Variability around the mean value was <50%. ^c Human umbilical vein endothelial cells. ^d ND = not determined.

It is well-documented in the literature that five-membered heteroaromatic rings, such as oxazoles and oxadiazoles, serve as excellent, hydrolytically stable bioisosteres for an ester substituent.^{29,30} As shown in Table 3, a series of methyl-substituted five-membered ring heterocycles was identified as acceptable replacements for the C6-ester or acid functionality of pyrrolo[2,1-*f*][1,2,4]triazine **14**. Oxazole **29** and 1,3,4-oxadiazole **37** demonstrated essentially equivalent VEGFR-2 kinase inhibitory activity compared to ester **14**, and both compounds inhibited FGFR-1 kinase activity with IC₅₀ values ca. 20 nM. The triazole **52** and the two regioisomeric 1,2,4 oxadiazole analogues **31** and **34** were less potent than **29** and **37** in the biochemical assays. The cellular potencies of **52** in the VEGF or FGF-driven HUVEC proliferation assays were consistent with the enzymatic activities obtained in the corresponding kinase assays. Compounds **29**, **31**, and **37** were significantly more potent inhibitors of HUVEC proliferation, regardless of the mitogen employed (IC₅₀ < 10 nM). Although the *in vitro* pharmacology of **29** was impressive, the oxazole analogue demonstrated significant activity against a panel of cytochrome (CYP) P450 isozymes (IC₅₀ values: CYP1A2, 0.064 μM; CYP2C9, 3.6 μM; and CYP3A4, 5.1 μM).

Since compound **37** provided an encouraging *in vitro* biological profile and an efficient synthesis of the 1,3,4-oxadiazole ring was available, the SAR of a series of substituted C6-oxadiazole analogues was investigated (Table 4). The unsubstituted oxadiazole **38** provided a significant reduction in biochemical and cellular potency compared to **37**, whereas substitution of the oxadiazole ring with larger aliphatic groups (i.e., **39–43**) was well-tolerated. Interestingly, while fluorination of the ethyl substituent of oxadiazole **39** did not significantly affect the kinase inhibitory activity for the two enzymes,

compound **46** demonstrated an order of magnitude decrease in cellular potency against VEGF- and FGF-stimulated HUVECs. Gradually increasing the electron-withdrawing capacity (higher σ value) of the R-substituent on the oxadiazole ring, as in the case of compounds **44** and **45**, provided a proportional decrease in biochemical potency and growth inhibition in the HUVEC proliferation assay. Alternatively, introduction of an electron-donating group, such as the dimethylamino substituent of compound **47**, led to improved potency in both the kinase and HUVEC proliferation assays. In an effort to optimize the ADME properties and enhance the aqueous solubility of the series, polar substituents, such as the dimethylaminomethyl and methylsulfonylmethyl groups, were appended to the oxadiazole core. Amine analogue **48** was less potent than methyloxadiazole **37** in the kinase assays; however, the sulfone derivative **49** afforded excellent biochemical and cellular potency. Consistent with previous results, the more electron deficient difluorosulfone oxadiazole **50** demonstrated comparable VEGFR-2 and FGFR-1 kinase activity to that of analogue **44** with IC₅₀ values of 53 and 220 nM, respectively. The cellular behavior of compound **50** in the VEGF- and FGF-simulated HUVEC proliferation assays was consistent with the biochemical data obtained for the two enzymes. To better understand the enzyme inhibitory properties of **50**, the K_i value was determined for VEGFR-2 kinase. Oxadiazole **50** was confirmed to be an ATP-competitive inhibitor of VEGFR-2, with an apparent K_i value of 52 ± 3 nM. The ability of the VEGFR-2 and FGFR-1 proteins to accommodate the diverse set of R groups illustrated in Table 4 again suggests that the C6-oxadiazole ring and appended substituents occupy a more flexible portion of the receptor that extends out toward solvent.

Proposed Binding Model for Compound 50. To better understand the binding mode of the 4-(5-(methoxycarbonyl)phenylamino)pyrrolo[2,1-*f*][1,2,4]triazines, a binding model of oxadiazole **50** in the ATP site of VEGFR-2 was developed using a reported crystal structure of the VEGFR-2 kinase domain.³⁷ Compound **50** was docked into the VEGFR-2 structure using the GLIDE software³⁸ and then energy-minimized with the CFF force field for 2000 steps of conjugate gradient minimization.³⁹ VEGFR-2 residues within 6 Å of the ligand were allowed to relax. Figure 2 depicts the proposed binding mode of **50** in the ATP binding pocket.

A highly conserved hydrogen-bond interaction between the backbone amide-NH of Cys919 and the N1 nitrogen of the pyrrolo[2,1-*f*][1,2,4]triazine ring anchors the inhibitor to the hinge region of the adenine binding pocket. The aniline portion of the inhibitor is oriented into a mostly hydrophobic pocket, deep within the binding site formed by residues such as Val916 and Leu889. The carbonyl and NH groups of the hydroxamate moiety form critical hydrogen bonds with the backbone NH of Asp1046 and the side chain of Glu885, respectively. The C5-isopropyl group makes van der Waals contacts with a hydrophobic cleft created by the proximal Val848 and Leu1035 residues. These same residues along with Cys1045 and Leu840 (not labeled in figure) roughly define the pocket occupied by the ribose ring of ATP. The oxadiazole heterocycle, while nearly coplanar with the pyrrolo[2,1-*f*][1,2,4]triazine

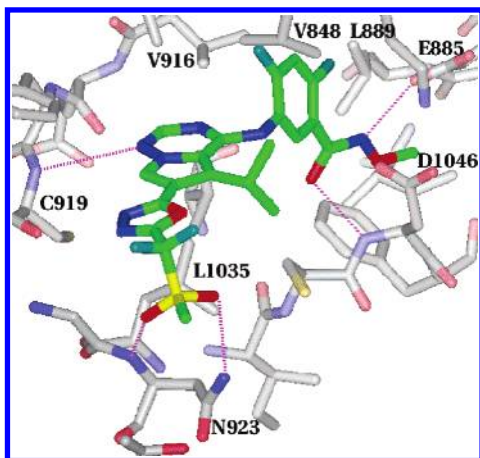


Figure 2. Binding model of compound **50** in the ATP binding site of VEGFR-2 kinase. Carbon atoms of **50** are in green and carbon atoms of the protein are in gray. Potential hydrogen-bond interactions are indicated by magenta dotted lines.

ring, points toward surface-exposed protein. Although not ultimately required for activity, the sulfone oxygen atoms likely form hydrogen bonds with the backbone NH and side chain of Asn923. In general, the binding model is consistent with the SAR and enzyme kinetics described above for the hydroxamate series.

Kinase Selectivity Profile for Select Analogues.

The most promising carbamate and oxadiazole analogues were screened against a representative panel of kinases, which included RTKs, non-RTKs, and serine/threonine kinases (Table 5). Since antiangiogenesis therapies target endothelial cells (of the host) rather than the tumor and preclinical efficacy studies are conducted in mice, Flk-1, the mouse homologue of human VEGFR-2 was also included in the panel. Compared to their VEGFR-2 inhibitory activity, a significant reduction in potency was observed for Flk-1, particularly for carbamate **24** (24-fold) and oxadiazoles **44** and **50** (8–15-fold). Although carbamate analogues **24** and **25** demonstrated single-digit micromolar activity against the HER-1 and HER-2 enzymes, the oxadiazole derivatives exhibited >150-fold selectivity for VEGFR-2 versus these epidermal growth factor receptor family members. Both the carbamate and oxadiazole analogues provided excellent VEGFR-2 kinase selectivity relative to other RTKs, such as PDGFR- β and IGF-1R. While maintaining reasonable selectivity for VEGFR-2 and FGFR-1 kinases (33- and 25-fold, respectively), oxadiazole **37** provided an IC_{50} = 500 nM against the non-RTK LCK. The other analogues depicted in Table 5 were considerably less potent against LCK. Similarly, no significant activity was detected with any of the hydroxamate-based, dual VEGFR-2 and FGFR-1 inhibitors versus the serine/threonine kinases PKC α and CDK2.

In Vitro Metabolic Stability and Pharmacokinetics. Several C6-carbamate and C6-heterocyclic pyrrolo[2,1-*f*][1,2,4]triazines with suitable inhibitory activity in the kinase and cellular proliferation assays were screened for metabolic stability in human liver microsomes (HLM). In general, the carbamate analogues exhibited a wide range of rates in this in vitro system (cf. Supporting Information). For example, incubation of the methyl sulfone, tetrahydrofuran, and *N*-methylpiperazinecarbamates **24–26** in HLM at 3 μ M for 10

min provided metabolic rates of 0.30, 0.074, and 0.104 nmol/min/mg protein, respectively. Moderate to high rates of drug conversion were obtained in HLM with the oxadiazole derivatives, which suggests the potential for high clearance in humans. Incubation of a 10 μ M concentration of the methyl sulfone oxadiazole **49** in HLM for 10 min provided a high metabolic rate of 0.60 nmol/min/mg protein. However, the HLM values for the fluorinated sulfone derivative **50** and the difluoromethyl analogue **44** were ca. 2-fold lower (0.27 and 0.35 nmol/min/mg protein, respectively), presumably due to removal of a potential site of oxidative metabolism.

To quickly assess the preliminary pharmacokinetic (PK) properties of this class of pyrrolo[2,1-*f*][1,2,4]-triazines, several carbamate and oxadiazole analogues were administered orally (50 mg/kg dose except for compound **50**) to male Balb/C mice and the plasma level concentrations were recorded at 1 and 4 h time points (Table 6). Carbamates **24–26** yielded relatively low drug exposures during the 4 h study. In contrast, oxadiazole analogues **37**, **44**, **49**, and **50** were all well-absorbed, producing remarkably high plasma level concentrations at the 1 h time point. Oxadiazoles **44** and **49** maintained high plasma exposures over the 4 h period, while the drug concentrations of compounds **50** and **37** decreased 2- and 3.5-fold, respectively.

Further assessment of the pharmacokinetics associated with compound **50** in Balb/C mice revealed that the steady-state volume of distribution (V_{ss}) was greater than total plasma/blood volume but less than total body water. These results are indicative of moderate extravascular distribution. The systemic plasma clearance (Cl) of compound **50** was less than 2% of hepatic blood flow. A 10 mg/kg oral dose administered as a solution in 3:1:6 poly(ethylene glycol):ethanol:water was readily absorbed and demonstrated a favorable half-life ($t_{1/2}$) and mean residence time (MRT). The measured oral bioavailability (F_{po}) of compound **50** in this study was 79%. The PK parameters from the comprehensive mouse study are summarized in Table 7. The plasma protein binding (PB) of compound **50** was calculated to be $99.8 \pm 0.04\%$ and $98.8 \pm 0.11\%$ in mouse and human serum, respectively, using the equilibrium dialysis method (at 10 μ M). Although the unbound (free) fraction available in mice was predicted to be low (0.2%), the favorable pharmacokinetic profile of **50** and the high plasma concentrations obtained with several analogues in the 4 h oral exposure studies warranted the advancement of these analogues into in vivo efficacy studies.

In Vivo Antitumor Activity. Four oxadiazole analogues were evaluated for antitumor efficacy in a L2987 human lung carcinoma xenograft model (Table 8). An active result in this study is defined as greater than 50% tumor growth inhibition (TGI) over at least one tumor volume doubling time (cf. Experimental Section). Compounds **37**, **44**, **49**, and **50** were administered orally for 10 consecutive days (qd \times 10) to nude mice bearing tumors staged to 100–150 mm³. Oxadiazole **37**, the most potent inhibitor of Flk-1 kinase activity (IC_{50} = 0.086 μ M), was toxic at the 50 mg/kg/day dose level in the L2987 model. However, administration of compound **37** at a 5-fold lower dose (10 mg/kg), twice daily for 20 consecutive days (2qd \times 20) provided good in vivo efficacy (79% TGI) in this model. Even with the signifi-

Table 5. Kinase Selectivity Profile for Select Carbamate and Oxadiazole Analogues^a

compd	enzyme inhibition IC ₅₀ (μM)									
	VEGFR-2	Flk-1	FGFR-1	HER-1	HER-2	PDGFR-β	IGF-1R	LCK	PKCα	CDK2
24	0.062	1.5	0.058	4.2	5.3	>2.0	>25	5.1	>50	>50
25	0.058	0.27	0.046	5.5	>10	>2.0	>25	4.7	>50	>50
37	0.018	0.086	0.019	>10	8.0	>2.0	>25	0.50	>50	>50
44	0.057	0.84	0.10	>10	>10	>2.0	>25	18	>50	>50
50	0.053	0.42	0.22	>25	>25	>2.0	>25	7.8	>50	>50

^a See Experimental Section for a description of assay conditions.

Table 6. Mouse Exposure Data Following Oral Administration of Select Compounds

compd	plasma levels (μM) ^{a,b}	
	at 1 h	at 4 h
24 ^c	7.9 ± 0.7	13.8 ± 2.1
25 ^c	29.5 ± 15.4	2.9 ± 1.5
26 ^c	5.1 ± 0.8	3.0 ± 0.9
37 ^c	131.6 ± 45.7	37.7 ± 17.0
44 ^c	187.4 ± 54.6	154.9 ± 63.1
49 ^c	287.8 ± 14.2	231.6 ± 23.8
50 ^d	26.6 ± 3.2	13.8 ± 1.0

^a Average of three male mice. ^b Vehicle: 3:1:6 PEG400/EtOH/water. ^c 50 mg/kg dose. ^d 10 mg/kg dose.

Table 7. Pharmacokinetic Properties of Compound **50** in Mice^{a,b}

parameter	unit	iv dose	po dose
dose	mg/kg	5	10
C _{max}	μM	23.7	27.7
T _{max}	h	—	0.5
AUC _{tot}	μM·h	97.4	155
t _{1/2}	h	2.5	3.6
MRT	h	4.9	5.2
Cl	mL/min/kg	1.53	—
V _{ss}	L/kg	0.45	—
F _{po}	%	—	79

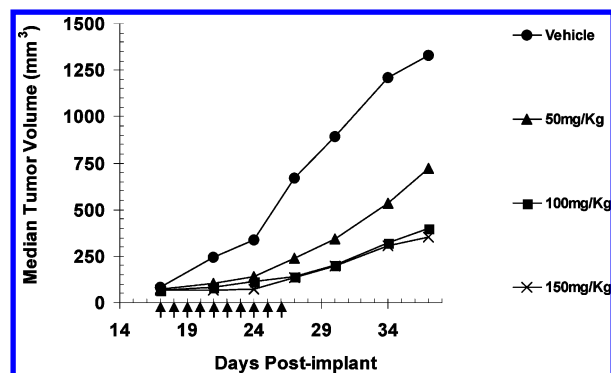
^a Composite serum concentration–time profiles were constructed for the PK analysis. ^b Vehicle: 3:1:6 PEG400/ethanol/water.

Table 8. Growth Inhibition for Oxadiazole Analogues against Established L2987 Human Lung Carcinoma Xenografts Implanted Subcutaneously in Athymic Mice

compd	dose (mg/kg/day) ^a	% TGI ^b
37	50	toxic ^c
	100	30.0
	150	46.5
44	50	88.4
	100	42.6
	150	74.9
49	50	63.9
	100	87.5
	150	94.2

^a Daily oral administration of compound for 10 consecutive days using 7:1:2 PEG 400/ethanol/water as the vehicle. ^b Maximum percent tumor growth inhibition over one tumor doubling time; >50% TGI is considered active in this study. ^c Compound **37** was active when dosed at 10 mg/kg/d on a 2qd × 20 schedule.

cant potency against Flk-1, the twice daily (2qd) dosing requirement for compound **37** may be a result of a considerable decline in plasma level concentrations following each dose, as observed in the 4 h oral exposure studies (vide supra). Analogues **44** and **49** exhibited antitumor activity at doses of 150 and 100 mg/kg/day, respectively, while compound **50**, provided robust *in vivo* efficacy at multiple dose levels. No overt toxicity (morbidity or weight loss) was observed with oxadiazole analogues **44**, **49**, and **50** at any dose level throughout

**Figure 3.** Antitumor activity of compound **50** against established L2987 human tumor xenografts implanted subcutaneously in athymic mice. Arrows indicate dosing (qd × 10).

the dosing regimen. The higher doses required for efficacy in this model with **44** and **50** may be attributed to the reduced Flk-1 activity of these compounds (IC₅₀ values of 0.84 and 0.42 μM) compared to oxazole **37** (IC₅₀ = 0.086 μM).

Figure 3 illustrates the dose-dependent growth inhibition of compound **50** in the L2987 tumor model. The two highest dose levels of 100 and 150 mg/kg/day provided similar antitumor activity (% TGI = 88 and 94%, respectively) with nearly complete tumor stasis throughout the dosing regimen (maximum efficacy). Consistent with the mechanisms of antiangiogenic therapy relative to VEGFR-2/FGFR-1 inhibition, tumor growth again commenced once compound dosing was terminated. Even at the low dose of 50 mg/kg/day, compound **50** was active, providing 64% tumor growth inhibition. A minimum effective dose for oxadiazole **50** was not established in this study.

Conclusions

Incorporation of the 2,4-difluoro-5-(methoxycarbonyl)phenylamino substituent at the C4-position of the pyrrolo[2,1-f][1,2,4]triazine scaffold resulted in potent and selective inhibitors of the VEGFR-2 and FGFR-1 kinases. In addition to the biochemical potency, many analogues demonstrated significant antiproliferative effects in growth factor-dependent HUVEC assays. Critical to the discovery of orally bioavailable analogues in the series were the SAR studies carried out at the 6-position of the pyrrolo[2,1-f][1,2,4]triazine nucleus. A survey of various C6-heterocycles led to the identification of substituted 1,3,5-oxadiazoles that served as metabolically stable bioisosteres for the C6-ester substituent. Preliminary assessment of the pharmacokinetic properties associated with compounds in the series revealed that the C6-carbamate analogues suffered from poor absorption, while several C6-heterocycles provided high exposures following oral administration in mice.

Further evaluation of oxadiazole **50** in mice showed that this compound possessed excellent oral bioavailability and a good half-life. The favorable in vitro pharmacology and pharmacokinetic properties exhibited by the oxadiazole analogues **44**, **49**, and **50** translated into significant antitumor activity in the L2987 human lung carcinoma xenograft model.

Experimental Section

Chemistry. All nonaqueous reactions were carried out under an argon or nitrogen atmosphere at room temperature, unless otherwise noted. All commercial reagents and anhydrous solvents were purchased from Aldrich and were used without further purification or distillation, unless otherwise stated. Analytical thin-layer chromatography (TLC) was performed on EM Science silica gel 60 F₂₅₄ (0.25 mm). Compounds were visualized by UV light and/or stained with either *p*-anisaldehyde, potassium permanganate, or cerium molybdate solutions followed by heating. Flash column chromatography was performed on EM Science silica gel 60 (particle size of 40–63 μm). Analytical high-pressure liquid chromatography (HPLC) and LC–MS analyses were conducted using Shimadzu LC-10AS pumps and a SPD-10AV UV–vis detector set at 220 nm with the MS detection performed with a Micromass Platform LC spectrometer. Analytical HPLC analyses were performed using one of the following conditions: column A, phenom-prime S5 C18 4.6 × 30 mm column; solvent A, 10% MeOH–90% H₂O–0.1% TFA; solvent B, 90% MeOH–10% H₂O–0.1% TFA; flow rate = 4 mL/min; linear gradient time = 2 min; start %B = 0, final %B = 100; or column B, Phenomenex Su C18 4.6 × 50 mm column; solvent A, 10% MeOH–90% H₂O–0.1% TFA; solvent B, 90% MeOH–10% H₂O–0.1% TFA; flow rate = 4 mL/min; linear gradient time = 4 min; start %B = 0, final %B = 100. Preparative reverse phase (RP) HPLC was performed using two Shimadzu LC-8A pumps, a SPD-10AV UV–vis detector set at 220 nm, and a YMC C18 ODS-A 5 μm, 20 × 100 mm column (eluting at 20 mL/min with a 12 min gradient of 0–100% B, where solvent A = 10% MeOH–90% H₂O–0.1% TFA and solvent B = 90% MeOH–10% H₂O–0.1% TFA). Following preparative HPLC purification, the fractions containing the desired product were concentrated under reduced pressure to remove the MeOH, neutralized with saturated aqueous NaHCO₃ to pH 7 and extracted with ethyl acetate (3 × 5 mL). The organic layers were dried (Na₂SO₄) and concentrated in vacuo to afford the desired compounds.

NMR (¹H and ¹³C) spectra were recorded on JEOL GSX 500 MHz or Bruker ARX 400 MHz spectrometers and calibrated using an internal reference. High-resolution mass spectra (HMRS) were recorded on a JEOL SX102 mass spectrometer. Elemental analyses were performed by Robertson Microlit Laboratories, and the results obtained are within ±0.4% of the theoretical values.

Diethyl 1-Amino-3-isopropyl-1H-pyrrole-2,4-dicarboxylate (4). To a solution of diethyl 3-isopropyl-1H-pyrrole-2,4-dicarboxylate²⁶ (**3**, 3.75 g, 14.8 mmol) in DMF (280 mL) at 0 °C was added NaH (60% dispersion in mineral oil, 0.890 g, 22.2 mmol) and the suspension was stirred for 10 min. *O*-(Diphenylphosphinyl)hydroxylamine (6.91 g, 29.6 mmol) was added to the reaction mixture and stirring was continued for 2 h. The reaction was quenched by the addition of pH 7 phosphate buffer (100 mL) and the mixture was extracted with EtOAc (4 × 100 mL). The combined EtOAc layers were dried (Na₂SO₄) and concentrated in vacuo. The residue was purified by flash chromatography (SiO₂, 20–25% EtOAc/hexanes gradient elution) to give **4** (3.38 g, 85%) as a white solid: Anal. RP-HPLC *t*_R = 1.29 min (column A, purity 97%); ¹H NMR (400 MHz, CDCl₃) δ 7.49 (s, 1H), 5.56 (s, 2H), 4.37 (q, 2H, *J* = 7.1 Hz), 4.32 (q, 2H, *J* = 7.1 Hz), 3.99 (hep, 1H, *J* = 7.2 Hz), 1.42–1.35 (m, 12H); MS (ESI) *m/z* 269 (M + H)⁺.

Ethyl 5-Isopropyl-4-oxo-3,4-dihydropyrrolo[2,1-*f*][1,2,4]-triazine-6-carboxylate (5). A solution of **4** (4.8 g, 18 mmol) in formamide (18 mL) was heated to 165 °C for 6 h and cooled

to room temperature. The resulting precipitate was filtered, washed with water, and dried overnight to afford **5** (4.0 g, 90%) as a white solid: Anal. RP-HPLC *t*_R = 1.56 min (column A, purity 99%); ¹H NMR (500 MHz, DMSO-*d*₆) δ 11.68 (s, 1H), 7.90 (s, 1H), 7.86 (d, 1H, *J* = 4.0 Hz), 4.24 (q, 2H, *J* = 7.1 Hz), 4.20 (m, 1H), 1.31 (d, 6H, *J* = 7.2 Hz), 1.29 (t, 3H, *J* = 7.1 Hz); ¹³C NMR (125 MHz, DMSO-*d*₆) δ 163.8, 155.0, 140.4, 134.7, 124.5, 117.6, 114.1, 60.1, 24.3, 21.8, 14.6; HRMS for C₁₂H₁₅N₃O₃ (M + H)⁺ calcd 250.1113, found 250.1102. Anal. (C₁₂H₁₅N₃O₃) C, H, N.

Ethyl 4-Chloro-5-isopropylpyrrolo[2,1-*f*][1,2,4]triazine-6-carboxylate (6). A mixture of **5** (17.8 g, 71.5 mmol), POCl₃ (12.0 g, 78.6 mmol), and a catalytic amount of Et₃N (1.00 mL, 7.15 mmol) in toluene (210 mL) was heated to reflux for 6 h and cooled to room temperature. The toluene was removed under reduced pressure. The residue was dissolved in CH₂Cl₂ and filtered through a pad of silica gel to give **6** (17.3 g, 90%) as a light yellow solid: Anal. RP-HPLC *t*_R = 1.95 min (column A, purity 95%); ¹H NMR (400 MHz, CDCl₃) δ 8.24 (s, 1H), 8.14 (s, 1H), 4.31 (hep, 1H, *J* = 7.2 Hz), 4.21 (q, 2H, *J* = 7.0 Hz), 1.46 (d, 6H, *J* = 7.2 Hz), 1.27 (t, 3H, *J* = 7.0 Hz).

Ethyl 5-Isopropyl-4-(3-(methoxycarbonyl)phenoxy)pyrrolo[2,1-*f*][1,2,4]triazine-6-carboxylate (8). To a solution of 3-hydroxybenzoic acid (0.69 g, 5.0 mmol) in THF (50 mL) were added EDCI (1.9 g, 10 mmol) and HOBt (1.4 g, 10 mmol) at room temperature. After 5 min, diisopropylethylamine (0.71 g, 5.5 mmol) and methyl hydroxylamine hydrochloride (0.63 g, 7.5 mmol) were added to the reaction, and the resulting mixture was stirred for 6 h. The reaction was diluted with EtOAc (150 mL) and washed with water (3 × 100 mL), 1 N HCl (1 × 50 mL), and brine (1 × 50 mL). The EtOAc layer was dried (Na₂SO₄) and concentrated in vacuo to give 3-hydroxy-*N*-methoxybenzamide (0.72 g, 86%), which was sufficiently pure to use in the subsequent step.

The crude 3-hydroxy-*N*-methoxybenzamide (25 mg, 0.15 mmol) was dissolved in DMF (2 mL) and treated with K₂CO₃ (21 mg, 0.15 mmol), and the resulting suspension was stirred at room temperature for 5 min. Ethyl 4-chloro-5-isopropylpyrrolo[2,1-*f*][1,2,4]triazine-6-carboxylate was added to the reaction and the mixture was stirred for 18 h. The resulting solid was filtered and washed with MeOH. The filtrate was concentrated in vacuo to give a yellow oil, which was dissolved in MeOH and purified by preparative HPLC to afford **8** (18 mg, 60%) as a clear film: Anal. RP-HPLC *t*_R = 1.89 min (column A, purity 98%); ¹H NMR (400 MHz, CD₃OD) δ 8.23 (s, 1H), 7.92 (s, 1H), 7.75 (d, 1H, *J* = 8.1 Hz), 7.69 (s, 1H), 7.60 (t, 1H, *J* = 8.1 Hz), 7.50 (d, 1H, *J* = 8.1 Hz), 4.37–4.31 (m, 3H), 3.82 (s, 3H), 1.48 (d, 6H, *J* = 7.1 Hz), 1.39 (t, 3H, *J* = 7.1 Hz); ¹³C NMR (125 MHz, CDCl₃) δ 164.2, 163.1, 151.5, 147.0, 137.4, 130.2, 130.0, 125.7, 124.8, 123.6, 121.7, 118.5, 117.0, 114.0, 64.8, 60.6, 25.2, 24.9, 21.5, 14.4; HRMS for C₂₀H₂₂N₄O₅ (M + H)⁺ calcd 399.1624, found 399.1679.

Ethyl 4-(2,4-Difluoro-5-(methoxycarbonyl)phenylamino)-5-isopropylpyrrolo[2,1-*f*][1,2,4]triazine-6-carboxylate (14). Representative Procedure for the Preparation of a *m*-Amino-*N*-methoxybenzamide Intermediate **7** and Subsequent Coupling to Ethyl 4-Chloro-5-isopropylpyrrolo[2,1-*f*][1,2,4]triazine-6-carboxylate. To a solution of 2,4-difluoro-5-nitrobenzoic acid⁴⁰ (5.00 g, 24.6 mmol) in EtOH (250 mL) was added tin chloride dihydrate (27.7 g, 123 mmol). The reaction mixture was heated to 50 °C for 10 min and then cooled to room temperature. EtOH was removed from the reaction mixture under reduced pressure. Ice water was added to the resulting residue, which was neutralized with saturated aqueous NaHCO₃ to pH 7 and extracted with EtOAc (3 × 300 mL). The organic layer was dried (Na₂SO₄) and concentrated in vacuo to give 5-amino-2,4-difluorobenzoic acid (3.20 g, 18.5 mmol, 75%), which was used directly in the subsequent reaction without further purification.

EDCI (9.45 g, 49.2 mmol) and HOBt (6.64 g, 49.2 mmol) were added to a solution of 5-amino-2,4-difluorobenzoic acid (4.26 g, 24.6 mmol) in THF (500 mL) and stirred at room temperature for 5 min. Diisopropyl ethylamine (3.30 g, 25.0 mmol) and methyl hydroxylamine hydrochloride (3.10 g, 37.5

mmol) were then added to the reaction and the mixture was stirred for 6 h. The reaction mixture was diluted with EtOAc (500 mL) and washed with saturated aqueous NaHCO₃ (3 × 200 mL), 1 N HCl (2 × 200 mL), and brine (1 × 200 mL). The EtOAc layer was dried (Na₂SO₄) and concentrated in vacuo. The resulting oil was purified by flash chromatography (SiO₂, 0–2% MeOH/CHCl₃ gradient elution) to give 5-amino-2,4-difluoro-*N*-methoxybenzamide (2.98 g, 14.8 mmol, 60%) as an off-white solid: Anal. RP-HPLC *t*_R = 0.97 min (column A, purity 99%); ¹H NMR (400 MHz, CD₃OD) δ 7.19 (dd, 1H, *J* = 7.0 Hz), 6.95 (t, 1H, *J* = 10.5 Hz), 3.81 (s, 3H); ¹³C NMR (125 MHz, CD₃OD) δ 163.5, 153.5 (dd, *J* = 247, 11 Hz), 152.5 (dd, *J* = 241, 10 Hz), 133.9 (d, *J* = 13 Hz), 117.4, 117.0 (d, *J* = 15 Hz), 104.6 (dd, *J* = 28, 26 Hz), 64.0; HRMS for C₈H₈F₂N₂O₂ (M – H)[–] calcd 201.0475, found 201.0474. Anal. (C₈H₈F₂N₂O₂) C, H, N.

A solution of 5-amino-*N*-methoxy-2,4-difluorobenzamide (20 mg, 0.10 mmol) and ethyl 4-chloro-5-isopropylpyrrolo[2,1-*f*][1,2,4]triazine-6-carboxylate (27 mg, 0.10 mmol) in DMF (2 mL) was stirred for 18 h. The crude reaction mixture was purified by preparative HPLC to afford **14** (34 mg, 78% yield) as a white solid: Anal. RP-HPLC *t*_R = 1.70 min (column A, purity 98%); ¹H NMR (400 MHz, CDCl₃) δ 9.42 (bs, 1H), 9.33 (bs, 1H), 8.18 (s, 1H), 7.60 (t, 1H, *J* = 10.4 Hz), 7.17 (t, 1H, *J* = 10.4 Hz), 4.40 (q, 2H, *J* = 7.2 Hz), 4.13 (hep, 1H, *J* = 7.2 Hz), 3.98 (s, 3H), 1.66 (d, 6H, *J* = 7.2 Hz), 1.50 (t, 3H, *J* = 7.2 Hz); HRMS for C₂₀H₂₁F₂N₅O₄ (M + H)⁺ calcd 434.1962, found 434.1965.

Ethyl 5-Isopropyl-4-(3-(methoxycarbamoyl)phenylamino)pyrrolo[2,1-*f*][1,2,4]triazine-6-carboxylate (9): clear film; Anal. RP-HPLC *t*_R = 1.88 min (column A, purity 97%); ¹H NMR (400 MHz, CD₃OD) δ 8.33 (s, 1H), 7.95 (s, 1H), 7.92–7.88 (m, 1H), 7.81 (s, 1H), 7.73–7.69 (m, 2H), 4.35 (q, 2H, *J* = 7.0 Hz), 3.89–3.78 (m, 4H), 1.55 (d, 6H, *J* = 7.2 Hz), 1.39 (t, 3H, *J* = 7.0 Hz); ¹³C NMR (125 MHz, CDCl₃ with 1 drop CD₃OD) δ 165.6, 163.7, 150.9, 150.4, 141.2, 138.5, 134.0, 130.4, 128.2, 126.7, 123.8, 121.6, 116.8, 110.7, 63.9, 60.9, 26.5, 24.7, 21.8, 14.0; HRMS for C₂₀H₂₃N₅O₄ (M + H)⁺ calcd 398.1828, found 398.1821.

Ethyl 5-Isopropyl-4-(3-(methoxycarbamoyl)-4-methylphenylamino)pyrrolo[2,1-*f*][1,2,4]triazine-6-carboxylate (10): clear film; Anal. RP-HPLC *t*_R = 1.68 min (column A, purity 98%); ¹H NMR (400 MHz, CD₃OD) δ 8.08 (s, 1H), 7.69 (s, 1H), 7.43–7.38 (m, 3H), 4.34 (q, 2H, *J* = 7.0 Hz), 3.98 (hep, 1H, *J* = 7.1 Hz), 3.84 (s, 3H), 2.45 (s, 3H), 1.51 (d, 6H, *J* = 7.1 Hz), 1.38 (t, 3H, *J* = 7.0 Hz); HRMS for C₂₁H₂₅N₅O₄ (M + H)⁺ calcd 412.1947, found 412.1984.

Ethyl 4-(4-Bromo-3-(methoxycarbamoyl)phenylamino)-5-isopropylpyrrolo[2,1-*f*][1,2,4]triazine-6-carboxylate (11): off-white solid; Anal. RP-HPLC *t*_R = 1.76 min (column A, purity 97%); ¹H NMR (400 MHz, CD₃OD) δ 7.95 (s, 1H), 7.68 (d, 1H, *J* = 8.6 Hz), 7.61 (s, 1H), 7.41 (s, 1H), 7.33 (d, 1H, *J* = 6.9 Hz), 4.31 (q, 2H, *J* = 7.1 Hz), 4.12 (hep, 1H, *J* = 7.0 Hz), 3.85 (s, 3H), 1.47 (d, 6H, *J* = 7.0 Hz), 1.40 (t, 3H, *J* = 7.1 Hz); HRMS for C₂₀H₂₂BrN₅O₄ (M + H)⁺ calcd 476.0933, found 476.0930.

Ethyl 4-(4-Fluoro-3-(methoxycarbamoyl)phenylamino)-5-isopropylpyrrolo[2,1-*f*][1,2,4]triazine-6-carboxylate (12): off-white solid; Anal. RP-HPLC *t*_R = 1.80 min (column A, purity 97%); ¹H NMR (400 MHz, CDCl₃) δ 9.35 (bs, 1H), 8.14–8.12 (m, 2H), 8.06 (s, 1H), 7.95 (s, 1H), 7.43 (bs, 1H), 7.21 (t, 1H, *J* = 10.1 Hz), 4.35 (q, 2H, *J* = 7.1 Hz), 4.13 (hep, 1H, *J* = 7.2 Hz), 3.92 (s, 3H), 1.57 (d, 6H, *J* = 7.2 Hz), 1.40 (t, 3H, *J* = 7.1 Hz); HRMS for C₂₀H₂₂FN₅O₄ (M + H)⁺ calcd 416.1734, found 416.1737.

Ethyl 4-(2-Fluoro-5-(methoxycarbamoyl)phenylamino)-5-isopropylpyrrolo[2,1-*f*][1,2,4]triazine-6-carboxylate (13): off-white solid; Anal. RP-HPLC *t*_R = 1.77 min (column A, purity 96%); ¹H NMR (400 MHz, CDCl₃) δ 9.09 (bs, 1H), 8.81 (bs, 1H), 8.07 (s, 1H), 8.04 (s, 1H), 7.75–7.73 (m, 1H), 7.60–7.56 (m, 1H), 7.25 (t, 1H, *J* = 10.5 Hz), 4.35 (q, 2H, *J* = 7.1 Hz), 4.17–4.11 (m, 1H), 3.93 (s, 3H), 1.55 (d, 6H, *J* = 7.3 Hz), 1.40 (t, 3H, *J* = 7.1 Hz); HRMS for C₂₀H₂₂FN₅O₄ (M + H)⁺ calcd 416.1734, found 416.1737.

Ethyl 4-(2,4-Difluoro-5-(ethoxycarbamoyl)phenylamino)-5-isopropylpyrrolo[2,1-*f*][1,2,4]triazine-6-carboxylate (15): colorless oil; Anal. RP-HPLC *t*_R = 1.80 min (column A, purity 98%); ¹H NMR (500 MHz, CDCl₃) δ 9.21 (bs, 1H), 9.08 (bs, 1H), 8.07 (s, 1H), 8.01 (s, 1H), 7.48 (s, 1H), 7.04 (t, 1H, *J* = 10.4 Hz), 4.38–4.31 (m, 2H), 4.19–4.08 (m, 3H), 1.55 (d, 6H, *J* = 7.2 Hz), 1.41–1.33 (m, 6H); ¹³C NMR (125 MHz, CDCl₃) δ 164.4, 160.9, 156.2 (dd, *J* = 242, 11 Hz), 155.7 (dd, *J* = 242, 11 Hz), 153.4, 147.8, 126.8 (d, *J* = 15 Hz), 126.5, 123.5, 123.2, 115.7 (d, *J* = 15 Hz), 115.4, 112.4, 104.4 (dd, *J* = 32, 26 Hz), 72.7, 60.5, 25.5, 22.7 (2C), 14.3, 13.5; HRMS for C₂₁H₂₃F₂N₅O₄ (M + H)⁺ calcd 448.1796, found 448.1782.

Ethyl 4-(2,4-Difluoro-5-(isopropoxycarbamoyl)phenylamino)-5-isopropylpyrrolo[2,1-*f*][1,2,4]triazine-6-carboxylate (16): off-white solid; Anal. RP-HPLC *t*_R = 3.84 min (column B, purity 98%); ¹H NMR (500 MHz, DMSO-*d*₆) δ 8.99 (bs, 1H), 8.12 (s, 1H), 7.85 (s, 1H), 7.49 (s, 1H), 7.38 (t, 1H, *J* = 10.5 Hz), 7.13 (t, 1H, *J* = 7.3 Hz), 4.83–4.49 (m, 1H), 4.18 (q, 1H, *J* = 7.0 Hz), 4.09 (hep, 1H, *J* = 7.2 Hz), 1.39–1.33 (m, 9H), 1.16 (d, 6H, *J* = 7.2 Hz); ¹³C NMR (125 MHz, DMSO-*d*₆) δ 163.6, 160.7, 155.5 (dd, *J* = 245, 10 Hz), 154.0 (dd, *J* = 240, 10 Hz), 149.0, 141.4, 139.0, 132.3 (d, *J* = 15 Hz), 124.2, 118.1, 117.0 (d, *J* = 15 Hz), 115.6, 112.0, 104.4 (t, *J* = 30 Hz), 76.8, 59.7, 24.2, 22.8, 22.1, 21.1, 20.6, 14.3; HRMS for C₂₂H₂₅F₂N₅O₄ (M + H)⁺ calcd 462.1953, found 462.1964.

Ethyl 4-(2,4-Difluoro-5-(isobutoxycarbamoyl)phenylamino)-5-isopropylpyrrolo[2,1-*f*][1,2,4]triazine-6-carboxylate (17): off-white solid; Anal. RP-HPLC *t*_R = 3.78 min (column B, purity 96%); ¹H NMR (500 MHz, CDCl₃) δ 9.21 (bs, 1H), 9.11 (bs, 1H), 8.07 (s, 1H), 8.01 (s, 1H), 7.49 (s, 1H), 7.02 (t, 1H, *J* = 8.0 Hz), 4.37–4.31 (m, 2H), 4.15 (hep, 1H, *J* = 7.2 Hz), 3.87–3.63 (m, 2H), 2.06–2.01 (m, 1H), 1.58–1.52 (m, 6H), 1.33 (t, 3H, *J* = 7.0 Hz), 1.06 (d, 6H, *J* = 6.9 Hz); ¹³C NMR (125 MHz, CDCl₃) δ 164.4, 160.7, 156.1 (dd, *J* = 247, 12 Hz), 155.5 (dd, *J* = 247, 12 Hz), 153.4, 147.8, 127.0, 126.5, 123.7 (d, *J* = 13 Hz), 123.2, 115.9 (d, *J* = 13 Hz), 115.4, 112.4, 104.3 (t, *J* = 28 Hz), 83.6, 60.5, 27.4, 25.5, 22.7 (2C), 19.2 (2C), 14.4; HRMS for C₂₃H₂₇F₂N₅O₄ (M + H)⁺ calcd 476.2109, found 476.2099.

Ethyl 4-(5-((Cyclopropylmethoxy)carbamoyl)-2,4-difluorophenylamino)-5-isopropylpyrrolo[2,1-*f*][1,2,4]triazine-6-carboxylate (18): off-white solid; Anal. RP-HPLC *t*_R = 3.81 min (column B, purity 98%); ¹H NMR (500 MHz, CDCl₃) δ 9.19–9.16 (m, 2H), 8.07 (s, 1H), 8.01 (s, 1H), 7.49 (s, 1H), 7.02 (t, 1H, *J* = 10.0 Hz), 4.34 (q, 2H, *J* = 7.1 Hz), 4.19–4.11 (m, 1H), 3.90 (d, 2H, *J* = 7.1 Hz), 1.55 (d, 6H, *J* = 7.7 Hz), 1.40 (t, 3H, *J* = 7.1 Hz), 1.29–1.18 (m, 1H), 0.68–0.61 (m, 2H), 0.39–0.33 (m, 2H); ¹³C NMR (125 MHz, CDCl₃) δ 164.4, 160.6, 156.4 (dd, *J* = 250, 14 Hz), 155.1 (dd, *J* = 250, 14 Hz), 153.4, 147.8, 127.0, 126.5, 123.5 (d, *J* = 11 Hz), 123.1, 115.4 (d, *J* = 17 Hz), 115.1, 112.2, 104.1 (t, *J* = 28 Hz), 81.5, 60.4, 25.4, 22.7 (2C), 14.3, 9.1, 3.1 (2C); HRMS for C₂₃H₂₅F₂N₅O₄ (M + H)⁺ calcd 474.1953, found 474.1956.

4-(2,4-Difluoro-5-(methoxycarbamoyl)phenylamino)-5-isopropylpyrrolo[2,1-*f*][1,2,4]triazine-6-carboxylic Acid (19). A mixture of compound **14** (6.0 g, 14 mmol) and 1 N NaOH (140 mL) in THF (140 mL) was heated to 60 °C for 27 h and then cooled to room temperature. The reaction mixture was acidified to pH 4 with 1 N HCl, and the volatiles were removed in vacuo. The precipitate was filtered, washed with diethyl ether, and dried under high vacuum overnight to give **19** (5.5 g, 98%) as an off-white solid: Anal. RP-HPLC *t*_R = 1.33 min (column A, purity 95%); ¹H NMR (400 MHz, DMSO-*d*₆) δ 12.28 (bs, 1H), 11.57 (s, 1H), 10.54 (s, 1H), 7.88 (s, 1H), 7.51–7.47 (m, 1H), 7.45 (t, 1H, *J* = 10.5 Hz), 7.22–7.18 (m, 1H), 4.46 (hep, 1H, *J* = 7.1 Hz), 3.70 (s, 3H), 1.34 (d, 6H, *J* = 7.1 Hz); MS (ESI) *m/z* 406 (M + H)⁺.

5-(6-(Azidocarbonyl)-5-isopropylpyrrolo[2,1-*f*][1,2,4]triazin-4-ylamino)-2,4-difluoro-*N*-methoxybenzamide (20). A solution of compound **19** (0.41 g, 0.94 mmol) in anhydrous 1,4-dioxane (10 mL) was treated with triethylamine (0.20 mL, 1.4 mmol) and diphenylphosphoryl azide (0.39 g, 1.4 mmol). The reaction mixture was heated to 40 °C for 1.5 h and then cooled to room temperature and concentrated under reduced

pressure. The residue was passed through a silica gel pad eluting with 25% EtOAc/hexanes to give **20** (0.42 g, 99%) as a pale yellow oil, which was used directly in the next step without further purification: Anal. RP-HPLC t_R = 1.86 min (column A, purity 90%); ^1H NMR (400 MHz, CDCl_3) δ 9.40 (bs, 1H), 9.10 (bs, 1H), 8.11 (s, 1H), 8.00 (s, 1H), 7.78 (s, 1H), 7.54 (t, 1H, J = 10.3 Hz), 4.15 (hep, 1H, J = 7.2 Hz), 3.91 (s, 3H), 1.60 (d, 6H, J = 7.2 Hz); MS (ESI) m/z 406 ($\text{M} + \text{H}^+$).

Ethyl 4-(2,4-Difluoro-5-(methoxycarbonyl)phenylamino)-5-isopropylpyrrolo[2,1-*f*][1,2,4]triazin-6-ylcarbamate (21). Representative Procedure for the Preparation of C6-Carbamate Derivatives. A mixture of compound **20** (50 mg, 0.12 mmol) and EtOH (53 mg, 1.2 mmol) in DMF (1.2 mL) was heated to 85 °C for 2 h. The reaction mixture was cooled to room temperature, concentrated under reduced pressure, and purified by flash chromatography (SiO_2 , 25–40% EtOAc/hexanes gradient elution) to give **21** (32 mg, 62%) as an amorphous solid: Anal. RP-HPLC t_R = 3.09 min (column B, purity 98%); ^1H NMR (500 MHz, CD_3OD) δ 8.01–7.97 (m, 1H), 7.62–7.58 (m, 2H), 7.02 (t, 1H, J = 10.1 Hz), 4.10 (q, 2H, J = 7.0 Hz), 3.72 (s, 3H), 3.58 (hep, 1H, J = 7.2 Hz), 1.35 (d, 6H, J = 7.2 Hz), 1.20 (q, 3H, J = 7.0 Hz); HRMS for $\text{C}_{20}\text{H}_{22}\text{F}_2\text{N}_6\text{O}_4$ ($\text{M} + \text{H}^+$)⁺ calcd 449.1749, found 449.1753.

Benzyl 4-(2,4-Difluoro-5-(methoxycarbonyl)phenylamino)-5-isopropylpyrrolo[2,1-*f*][1,2,4]triazin-6-ylcarbamate (22): amorphous solid; Anal. RP-HPLC t_R = 1.70 min (column A, purity 97%); ^1H NMR (400 MHz, CD_3OD) δ 7.98 (m, 1H), 7.71 (s, 1H), 7.40–7.18 (m, 6H), 7.12 (t, 1H, J = 10.0 Hz), 5.19 (s, 2H), 3.81 (s, 3H), 3.65 (hep, 1H, J = 7.2 Hz), 1.42 (d, 6H, J = 7.2 Hz); MS (ESI) m/z 511 ($\text{M} + \text{H}^+$)⁺.

3-(Piperidin-1-yl)propyl 4-(2,4-difluoro-5-(methoxycarbonyl)phenylamino)-5-isopropylpyrrolo[2,1-*f*][1,2,4]triazin-6-ylcarbamate, Hydrochloride Salt (23): amorphous solid; Anal. RP-HPLC t_R = 2.28 min (column B, purity 98%); ^1H NMR (500 MHz, CD_3OD) δ 8.05–7.99 (m, 1H), 7.62–7.58 (m, 2H), 7.22 (t, 1H, J = 10.1 Hz), 4.28–4.23 (m, 2H), 3.85 (s, 3H), 3.69–3.62 (m, 2H), 3.26–3.23 (m, 2H), 2.98–2.91 (m, 2H), 2.20–2.11 (m, 2H), 2.10–1.91 (m, 2H), 1.89–1.74 (m, 4H), 1.59–1.50 (m, 1H), 1.47 (d, 6H, J = 7.1 Hz); ^{13}C NMR (125 MHz, CDCl_3) δ 163.7, 162.2, 161.5, 158.0, 156.4 (dd, J = 251, 12 Hz), 155.1 (dd, J = 251, 12 Hz), 151.8, 145.5, 127.0 (d, J = 15 Hz), 124.4, 123.5, 115.1 (d, J = 15 Hz), 113.8, 104.4 (t, J = 28 Hz), 64.8, 61.9, 54.4, 53.4, 37.0, 34.9, 31.7, 25.7, 23.8, 23.3, 22.7, 22.0; HRMS for $\text{C}_{26}\text{H}_{33}\text{F}_2\text{N}_7\text{O}_4$ ($\text{M} + \text{H}^+$)⁺ calcd 546.2640, found 546.2616.

3-(Methylsulfonyl)propyl 4-(2,4-difluoro-5-(methoxycarbonyl)phenylamino)-5-isopropylpyrrolo[2,1-*f*][1,2,4]triazin-6-ylcarbamate (24): amorphous solid; Anal. RP-HPLC t_R = 2.51 min (column B, purity 98%); ^1H NMR (500 MHz, $\text{DMSO}-d_6$) δ 8.78 (s, 1H), 7.68–7.55 (m, 3H), 7.50–7.41 (m, 1H), 4.18–4.10 (m, 2H), 3.69 (s, 3H), 3.67–3.60 (m, 2H), 3.26–3.19 (m, 2H), 3.00 (s, 3H), 2.09–1.98 (m, 2H), 1.32 (d, 6H, J = 7.2 Hz); HRMS for $\text{C}_{22}\text{H}_{26}\text{F}_2\text{N}_6\text{O}_6\text{S}$ ($\text{M} + \text{H}^+$)⁺ calcd 541.1637, found 541.1635.

(Tetrahydrofuran-2-yl)methyl 4-(2,4-difluoro-5-(methoxycarbonyl)phenylamino)-5-isopropylpyrrolo[2,1-*f*][1,2,4]triazin-6-ylcarbamate (25): amorphous solid; Anal. RP-HPLC t_R = 2.91 min (column B, purity 98%); ^1H NMR (500 MHz, $\text{DMSO}-d_6$) δ 11.8 (bs, 1H), 8.84 (bs, 1H), 7.68–7.40 (m, 4H), 4.18–3.97 (m, 2H), 3.71 (s, 3H), 3.71–3.57 (m, 3H), 1.97–1.81 (m, 3H), 1.67–1.60 (m, 1H), 1.32 (d, 6H, J = 6.9 Hz); HRMS for $\text{C}_{23}\text{H}_{26}\text{F}_2\text{N}_6\text{O}_5$ ($\text{M} + \text{H}^+$)⁺ calcd 505.1936, found 505.1931.

Methylpiperidin-4-yl 4-(2,4-difluoro-5-(methoxycarbonyl)phenylamino)-5-isopropylpyrrolo[2,1-*f*][1,2,4]triazin-6-ylcarbamate, Hydrochloride Salt (26): amorphous solid; Anal. RP-HPLC t_R = 1.03 min (column A, purity 94%); ^1H NMR (500 MHz, CD_3OD) δ 8.38 (bs, 1H), 7.83 (s, 1H), 7.76 (s, 1H), 7.39–7.11 (m, 4H), 4.98–4.89 (m, 2H), 3.83 (s, 3H), 3.63–3.54 (m, 1H), 3.29–3.18 (m, 1H), 3.10–2.99 (m, 2H), 2.72 (s, 3H), 2.30–2.23 (m, 2H), 2.10–2.01 (m, 2H), 1.49 (bs, 6H); MS (ESI) m/z 518 ($\text{M} + \text{H}^+$)⁺.

5-Isopropyl-4-oxo-3,4-dihydropyrrolo[2,1-*f*][1,2,4]triazine-6-carboxylic Acid (27). A solution of ester **5** (4.0

g, 16 mmol) in THF/water (100/10 mL) was treated with 1 N NaOH (82 mL) and the resulting mixture was heated to 60 °C for 8 h, cooled to room temperature, and concentrated under reduced pressure to remove the THF. The remaining solution was acidified with 1 N HCl to pH 3. The precipitate was filtered, washed with water, and dried under high vacuum overnight to give **27** (3.4 g, 95%) as a white solid, which was used directly in the next step without further purification: Anal. RP-HPLC t_R = 2.30 min (column B, purity 98%); ^1H NMR (500 MHz, $\text{DMSO}-d_6$) δ 12.40 (bs, 1H), 11.63 (bs, 1H), 7.86 (s, 1H), 7.83 (s, 1H), 4.21 (hep, 1H, J = 7.1 Hz), 1.31 (d, 6H, J = 7.1 Hz); ^{13}C NMR (125 MHz, $\text{DMSO}-d_6$) δ 165.0, 154.6, 139.8, 134.4, 124.2, 117.1, 113.6, 23.7, 21.4 (2C); HRMS for $\text{C}_{10}\text{H}_{11}\text{N}_3\text{O}_3$ ($\text{M} - \text{H}^-$)⁻ calcd 220.0800, found 220.0728.

2,4-Difluoro-5-(5-isopropyl-6-(5-methyloxazol-2-yl)pyrrolo[2,1-*f*][1,2,4]triazin-4-ylamino)-*N*-methoxybenzamide (29). A mixture of acid **27** (0.44 g, 2.0 mmol), 1-aminoacetone HCl salt⁴¹ (0.27 g, 2.5 mmol), BOP reagent (1.1 g, 2.5 mmol), and triethylamine (0.68 mL, 4.9 mmol) in DMF (5 mL) was stirred at 50 °C for 2 h. The reaction mixture was partitioned between ethyl acetate (10 mL) and water (5 mL). The ethyl acetate layer was washed with brine, dried (MgSO_4), and concentrated under reduced pressure. The residue was then purified by flash chromatography (SiO_2 ; 100% ethyl acetate) to afford 4-hydroxy-5-isopropyl-*N*-(2-oxopropyl)pyrrolo[2,1-*f*][1,2,4]triazine-6-carboxamide (0.34 g, 61%) as a pale yellow solid, which was used directly in the next step.

The above carboxamide (55 mg, 0.21 mmol) was stirred with POCl_3 (2 mL) at 120 °C for 6 h. The excess POCl_3 was removed in vacuo and the residue was partitioned between dichloromethane (10 mL) and saturated aqueous NaHCO_3 solution (10 mL). The organic layer was dried (MgSO_4) and concentrated under reduced pressure. The residue was purified by flash chromatography (SiO_2 , 50% ethyl acetate/hexane) to afford chloroimidate **28** (31 mg, 0.11 mmol, 55%) as a pale yellow oil: Anal. RP-HPLC t_R = 1.87 min (column A, purity 98%); ^1H NMR (400 MHz, CDCl_3) δ 8.30 (s, 1H), 8.12 (s, 1H), 6.90 (s, 1H), 4.33 (hep, 1H, J = 7.2 Hz), 2.41 (s, 3H), 1.46 (d, 6H, J = 7.2 Hz).

A solution of **28** (31 mg, 0.11 mmol) and 5-amino-2,4-difluoro-*N*-methoxybenzamide (24 mg, 0.12 mmol) in MeCN (3 mL) was stirred at room temperature for 18 h. The solvent was removed under reduced pressure and the residue was purified by preparative HPLC to afford **29** (42 mg, 86%) as a white solid: Anal. RP-HPLC t_R = 1.71 min (column A, purity 97%); ^1H NMR (500 MHz, CD_3OD) δ 7.80 (s, 1H), 7.71–7.66 (m, 1H), 7.49 (s, 1H), 7.14 (t, 1H, J = 10.1 Hz), 6.86 (s, 1H), 4.04 (hep, 1H, J = 7.2 Hz), 3.24 (s, 3H), 2.33 (s, 3H), 1.35 (d, 6H, J = 7.0 Hz); ^{13}C NMR (125 MHz, CDCl_3) δ 160.9, 157.1, 156.5 (dd, J = 248, 10 Hz), 155.5 (dd, J = 250, 10 Hz), 152.8, 148.1, 147.1, 146.8, 126.8, 123.8, 122.9, 119.6, 115.0 (d, J = 12 Hz), 113.3, 112.1, 105.5 (dd, J = 29, 27 Hz), 64.8, 25.4, 23.0 (2C), 10.9; HRMS for $\text{C}_{21}\text{H}_{26}\text{F}_2\text{N}_6\text{O}_3$ ($\text{M} + \text{H}^+$)⁺ calcd 443.1643, found 443.1648.

2,4-Difluoro-5-(5-isopropyl-6-(3-methyl-1,2,4-oxadiazol-5-yl)pyrrolo[2,1-*f*][1,2,4]triazin-4-ylamino)-*N*-methoxybenzamide (31). To a solution of acid **27** (0.20 g, 0.90 mmol), *N*-hydroxybenzotriazole (24 mg, 0.018 mmol), and diisopropylethylamine (0.58 g, 4.5 mmol) in DMF (9 mL) was added benzotriazol-1-yl-*N,N,N',N'*-tetramethyluronium tetrafluoroborate (0.29 g, 0.90 mmol) at room temperature. *N*-Hydroxylacetamide was added to the reaction and the resulting mixture was stirred for 14 h. The reaction mixture was quenched with water (7 mL) and extracted with EtOAc (3 × 10 mL). The EtOAc layers were washed with 10% aqueous LiCl (2 × 5 mL), dried (Na_2SO_4), and concentrated under reduced pressure to give the desired intermediate, which was used directly in the next step without further purification: MS (ESI) m/z 278 ($\text{M} + \text{H}^+$)⁺.

The above intermediate was dissolved in DMF (9 mL) and heated to 140 °C for 3 h. The reaction mixture was cooled to room temperature, diluted with EtOAc (30 mL), and washed with 10% aqueous LiCl (3 × 50 mL). The organics were dried (Na_2SO_4), concentrated in vacuo, and triturated with 10%

MeOH in Et₂O to give **30** (0.13 g, 0.51 mmol, 57%) as a white solid: Anal. RP-HPLC *t_R* = 1.59 min (column A, purity 98%); ¹H NMR (400 MHz, DMSO-*d*₆) δ 11.79 (bs, 1H), 8.25 (s, 1H), 7.92 (s, 1H), 4.18 (hep, 1H, *J* = 7.2 Hz), 2.50 (s, 3H), 1.37 (d, 6H, *J* = 7.2 Hz); MS (ESI) *m/z* 260 (M + H)⁺.

Intermediate **30** (65 mg, 0.25 mmol) was treated with POCl₃ (2 mL) at 120 °C for 6 h. The excess POCl₃ was removed under reduced pressure and the residue was coevaporated with toluene. The residue was then dissolved in MeCN (3 mL) and treated with 5-amino-2,4-difluoro-*N*-methoxybenzamide (51 mg, 0.25 mmol). The reaction mixture was stirred at room temperature for 18 h. The solvent was removed under reduced pressure and the residue was purified by preparative HPLC to afford **31** (73 mg, 68%) as an off-white solid: Anal. RP-HPLC *t_R* = 3.11 min (column B, purity 98%); ¹H NMR (500 MHz, CD₃OD) δ 8.24 (s, 1H), 7.86–7.81 (m, 1H), 7.68 (s, 1H), 7.32 (t, 1H, *J* = 10.5 Hz), 4.11–4.07 (m, 1H), 3.78 (s, 3H), 2.40 (s, 3H), 1.47 (d, 6H, *J* = 6.6 Hz); ¹³C NMR (125 MHz, CD₃OD) δ 171.8, 166.7, 159.8, 156.6 (dd, *J* = 250, 10 Hz), 154.5 (dd, *J* = 245, 10 Hz), 140.9, 138.7, 132.3, 131.5, 124.5, 122.1, 117.8, 115.3 (d, *J* = 15 Hz), 113.7, 105.2 (t, *J* = 28 Hz), 63.0, 24.4, 20.8 (2C), 11.0; HRMS for C₂₀H₁₉F₂N₇O₃ (M + H)⁺ calcd 444.1596, found 444.1590.

5-Isopropyl-4-oxo-3,4-dihydropyrrolo[2,1-*f*][1,2,4]-triazine-6-carbonitrile (32). A mixture of acid **27** (0.39 g, 1.8 mmol), concentrated NH₄OH (2 mL), EDCI (0.44 g, 2.3 mmol), and HOBt (0.26 g, 1.9 mmol) in DMF (8 mL) was stirred at room temperature for 4 h. The reaction mixture was diluted with water (10 mL) and extracted with EtOAc (3 × 20 mL). The EtOAc layer was dried (Na₂SO₄), concentrated under reduced pressure, and triturated with diethyl ether to give 5-isopropyl-4-oxo-3,4-dihydropyrrolo[2,1-*f*][1,2,4]triazine-6-carboxamide (0.36 g, 92%) as an off-white solid: Anal. RP-HPLC *t_R* = 1.60 min (column A, purity 90%); MS (ESI) *m/z* 221 (M + H)⁺.

The above amide (60 mg, 0.27 mmol) was dissolved in POCl₃ (1 mL), heated to 60 °C under N₂ for 1 h, and then cooled to room temperature. The POCl₃ was removed under reduced pressure and coevaporated with toluene. The residue was dissolved in EtOAc (5 mL) and washed with saturated aqueous NaHCO₃. The organics were dried (Na₂SO₄), concentrated in vacuo, and triturated with 10% MeOH in diethyl ether to afford compound **32** (50 mg, 88%) as an off-white solid: Anal. RP-HPLC *t_R* = 1.45 min (column A, purity 90%); ¹H NMR (400 MHz, DMSO-*d*₆) δ 7.56 (s, 1H), 7.23 (s, 1H), 4.21 (hep, 1H, *J* = 7.2 Hz), 1.31 (d, 6H, *J* = 7.2 Hz); MS (ESI) *m/z* 201 (M + H)⁺.

2,4-Difluoro-5-(5-isopropyl-6-(5-methyl-1,2,4-oxadiazol-3-yl)pyrrolo[2,1-*f*][1,2,4]triazin-4-ylamino)-*N*-methoxybenzamide (34). A mixture of compound **32** (70 mg, 0.35 mmol), hydroxylamine hydrochloride (37 mg, 1.0 mmol), and K₂CO₃ (0.23 g, 1.7 mmol) in EtOH (4 mL) was heated to reflux for 28 h and then cooled to room temperature. Water (4 mL) was added to the reaction and the mixture was extracted with EtOAc (3 × 10 mL). The combined EtOAc layers were washed with brine (1 × 10 mL), dried (Na₂SO₄), and concentrated under reduced pressure to give *N*'-hydroxy-5-isopropyl-4-oxo-3,4-dihydropyrrolo[2,1-*f*][1,2,4]triazine-6-carboximidine, which was used directly in the next step without further purification: Anal. RP-HPLC *t_R* = 1.38 min (column A, purity 90%); MS (ESI) *m/z* 335 (M + H)⁺.

The above amidine was dissolved in pyridine (2 mL) and treated with acetyl chloride (0.5 mL). The reaction mixture was heated to reflux for 7 h, cooled to room temperature, diluted with water (4 mL), and extracted with EtOAc (3 × 10 mL). The organic layers were washed with 1 N NaOH (1 × 5 mL) and 1 N HCl (2 × 5 mL), dried (Na₂SO₄), concentrated in vacuo, and purified by flash chromatography (SiO₂, 5–10% MeOH/CH₂Cl₂ gradient elution) to give **33** (10 mg, 0.039 mmol, 11%) as an off-white solid: Anal. RP-HPLC *t_R* = 1.25 min (column A, purity 98%); ¹H NMR (400 MHz, DMSO-*d*₆) δ 8.20 (s, 1H), 7.91 (s, 1H), 4.11 (hep, 1H, *J* = 7.2 Hz), 2.47 (s, 3H), 1.37 (d, 6H, *J* = 7.2 Hz); MS (ESI) *m/z* 260 (M + H)⁺.

Compound **33** (10 mg, 0.039 mmol) was dissolved in POCl₃ (1 mL) and the resulting mixture was heated at 120 °C for 5 h. The excess POCl₃ was removed under reduced pressure and the residue was coevaporated with toluene. The residue was then dissolved in MeCN and treated with 5-amino-2,4-difluoro-*N*-methoxybenzamide (8.0 mg, 0.040 mmol) and the mixture was stirred at room temperature for 14 h. The solvent was removed under reduced pressure and the residue was purified by preparative HPLC to afford **34** (5.2 mg, 30%) as an off-white solid: Anal. RP-HPLC *t_R* = 1.49 min (column A, purity 98%); ¹H NMR (400 MHz, DMSO-*d*₆) δ 11.60 (s, 1H), 7.88 (s, 1H), 7.58 (s, 1H), 7.48 (t, 1H, *J* = 10.4 Hz), 7.31 (m, 1H), 5.5 (bs, 1H), 4.25 (hep, 1H, *J* = 7.2 Hz), 3.71 (s, 3H), 2.65 (s, 3H), 1.39 (d, 6H, *J* = 7.2 Hz); ¹³C NMR (125 MHz, CD₃OD) δ 178.5, 163.4, 160.4, 155.0 (dd, *J* = 250, 10 Hz), 154.5 (dd, *J* = 245, 10 Hz), 140.9, 138.7, 132.3, 131.5, 123.0 (d, *J* = 10 Hz), 122.1, 117.8, 115.3 (d, *J* = 15 Hz), 113.7, 105.5 (t, *J* = 30 Hz), 63.0, 26.4, 22.3 (2C), 14.5; HRMS for C₂₀H₁₉F₂N₇O₃ (M + H)⁺ calcd 444.1596, found 444.1580.

5-Isopropyl-4-oxo-3,4-dihydropyrrolo[2,1-*f*][1,2,4]-triazine-6-carbohydrazide (35). A mixture of ester **5** (20.0 g, 80.3 mmol), hydrazine (80 mL), and EtOH (20 mL) was heated to 90 °C for 4 h, cooled to room temperature, and concentrated under reduced pressure. The residue was triturated with 10% MeOH/Et₂O to give **35** (17.9 g, 95%) as an off-white solid: Anal. RP-HPLC *t_R* = 0.72 min (column A, purity 95%); ¹H NMR (400 MHz, DMSO-*d*₆) δ 9.30 (bs, 1H), 7.78 (s, 1H), 7.76 (s, 1H), 4.36–4.11 (bs, 3H), 4.08 (hep, 1H, *J* = 7.2 Hz), 1.30 (d, 6H, *J* = 7.2 Hz); MS (ESI) *m/z* 236 (M + H)⁺.

2,4-Difluoro-5-(5-isopropyl-6-(5-methyl-1,3,4-oxadiazol-2-yl)pyrrolo[2,1-*f*][1,2,4]triazin-4-ylamino)-*N*-methoxybenzamide (37). Representative Procedure for the Preparation of Chloroimidate **36** and Subsequent Coupling to 5-Amino-2,4-difluoro-*N*-methoxybenzamide. A mixture of hydrazide **35** (0.10 g, 0.43 mmol) and the corresponding carboxylic acid (acetic acid, 0.2 mL) in POCl₃ (2 mL) was heated to 100 °C for 1 h and then at 120 °C for 3 h under N₂. The reaction mixture was cooled to room temperature. The POCl₃ was removed under reduced pressure and coevaporated with toluene. The residue was dissolved in EtOAc (5 mL) and washed with cold saturated aqueous NaHCO₃. The EtOAc layer was dried (Na₂SO₄) and passed through a short silica gel pad to give 4-chloro-5-isopropyl-6-(5-methyl-1,3,4-oxadiazol-2-yl)-pyrrolo[2,1-*f*][1,2,4]triazine (**36**), which was used directly in the next step without further purification.

4-Chloro-5-isopropyl-6-(5-methyl-1,3,4-oxadiazol-2-yl)pyrrolo[2,1-*f*][1,2,4]triazine (**36**, 33 mg, 0.11 mmol) was treated with 5-amino-2,4-difluoro-*N*-methoxybenzamide (24 mg, 0.12 mmol) in DMF (3 mL) and the mixture was stirred at 50 °C for 6 h. The solvent was removed in vacuo and the residue was purified by preparative HPLC to afford **37** (30 mg, 60%) as a white solid: Anal. RP-HPLC *t_R* = 1.58 min (column A, purity 98%); ¹H NMR (400 MHz, CD₃OD) δ 8.25 (s, 1H), 7.96–7.92 (m, 1H), 7.78 (s, 1H), 7.41 (t, 1H, *J* = 10.0 Hz), 4.08 (hep, 1H, *J* = 7.1 Hz), 3.85 (s, 3H), 2.65 (s, 3H), 1.54 (d, 6H, *J* = 7.1 Hz); HRMS for C₂₀H₁₉F₂N₇O₃ (M + H)⁺ calcd 444.1596, found 444.1599.

5-(6-(5-Ethyl-1,3,4-oxadiazol-2-yl)-5-isopropylpyrrolo[2,1-*f*][1,2,4]triazin-4-ylamino)-2,4-difluoro-*N*-methoxybenzamide (39): off-white solid; Anal. RP-HPLC *t_R* = 1.69 min (column A, purity 96%); ¹H NMR (400 MHz, CD₃OD) δ 7.98 (s, 1H), 7.76–7.73 (m, 1H), 7.58 (s, 1H), 7.25 (t, 1H, *J* = 10.1 Hz), 4.24 (hep, 1H, *J* = 7.1 Hz), 3.85 (s, 3H), 3.00 (q, 2H, *J* = 7.5 Hz), 1.49 (d, 6H, *J* = 7.1 Hz), 1.44 (t, 3H, *J* = 7.5 Hz); HRMS for C₂₁H₂₁F₂N₇O₃ (M + H)⁺ calcd 458.1698, found 458.1699.

2,4-Difluoro-5-(5-isopropyl-6-(5-isopropyl-1,3,4-oxadiazol-2-yl)pyrrolo[2,1-*f*][1,2,4]triazin-4-ylamino)-*N*-methoxybenzamide (40): off-white solid; Anal. RP-HPLC *t_R* = 1.76 min (column A, purity 98%); ¹H NMR (400 MHz, CDCl₃) δ 9.26–9.21 (m, 2H), 8.07 (s, 1H), 8.06 (s, 1H), 7.53–7.51 (m, 1H), 7.06 (t, 1H, *J* = 10.3 Hz), 4.26–4.22 (m, 1H), 3.94 (s, 3H), 3.32–3.25 (m, 1H), 1.57 (d, 6H, *J* = 7.3 Hz), 1.46 (d, 6H, *J* = 7.1 Hz); HRMS for C₂₂H₂₃F₂N₇O₃ (M + H)⁺ calcd 472.1888, found 472.1890.

2,4-Difluoro-5-(6-(5-isobutyl-1,3,4-oxadiazol-2-yl)-5-isopropylpyrrolo[2,1-f][1,2,4]triazin-4-ylamino)-N-methoxybenzamide (41): off-white solid; Anal. RP-HPLC t_R = 1.87 min (column A, purity 95%); ^1H NMR (400 MHz, CD_3OD) δ 7.95 (s, 1H), 7.74–7.72 (m, 1H), 7.57 (s, 1H), 7.24 (t, 1H, J = 10.1 Hz), 4.26–4.22 (m, 1H), 3.84 (s, 3H), 2.86 (d, 2H, J = 7.1 Hz), 2.28–2.21 (m, 1H), 1.49 (d, 6H, J = 7.1 Hz), 1.08 (d, 6H, J = 6.7 Hz); HRMS for $\text{C}_{23}\text{H}_{25}\text{F}_2\text{N}_7\text{O}_3$ ($\text{M} + \text{H}$) $^+$ calcd 486.1202, found 486.1204.

5-(6-(5-Cyclopropyl-1,3,4-oxadiazol-2-yl)-5-isopropylpyrrolo[2,1-f][1,2,4]triazin-4-ylamino)-2,4-difluoro-N-methoxybenzamide (42): off-white solid; Anal. RP-HPLC t_R = 3.57 min (column B, purity 98%); ^1H NMR (500 MHz, CDCl_3) δ 9.27–9.22 (m, 2H), 8.03–8.01 (m, 2H), 7.58–7.50 (m, 1H), 7.05 (t, 1H, J = 10.1 Hz), 4.28–4.21 (m, 1H), 3.93 (s, 3H), 2.26–2.22 (m, 1H), 1.55 (d, 6H, J = 7.1 Hz), 1.24–1.18 (m, 4H); ^{13}C NMR (125 MHz, CDCl_3) δ 167.8, 160.8, 160.5, 156.2 (dd, J = 250, 14 Hz), 155.7 (dd, J = 254, 14 Hz), 152.9, 147.5, 127.0, 123.7 (d, J = 41 Hz), 119.9 (2C), 115.6 (d, J = 15 Hz), 112.8, 109.0, 104.5 (dd, J = 30, 27 Hz), 64.8, 43.5, 25.9, 22.8, 8.6 (2C), 6.4; HRMS for $\text{C}_{22}\text{H}_{21}\text{F}_2\text{N}_7\text{O}_3$ ($\text{M} + \text{H}$) $^+$ calcd 470.1752, found 470.1756.

5-(6-(5-(Cyclopropylmethyl)-1,3,4-oxadiazol-2-yl)-5-isopropylpyrrolo[2,1-f][1,2,4]triazin-4-ylamino)-2,4-difluoro-N-methoxybenzamide (43): off-white solid; Anal. RP-HPLC t_R = 3.50 min (column B, purity 98%); ^1H NMR (400 MHz, CDCl_3) δ 9.31–9.26 (m, 1H), 9.13 (bs, 1H), 8.07–7.93 (m, 2H), 7.46 (bs, 1H), 6.97 (t, 1H, J = 10.2 Hz), 4.21–4.17 (m, 1H), 3.85 (s, 3H), 2.77 (d, 2H, J = 7.1 Hz), 1.49 (d, 6H, J = 7.1 Hz), 1.17–1.09 (m, 1H), 0.61–0.56 (m, 2H), 0.31–0.27 (m, 2H); ^{13}C NMR (100 MHz, $\text{DMSO}-d_6$) δ 166.2, 161.5, 161.2, 160.1, 156.5 (dd, J = 250, 10 Hz), 154.5 (dd, J = 245, 10 Hz), 153.5, 147.5, 129.9, 127.0, 124.5 (d, J = 10 Hz), 119.9, 117.8, 116.3 (d, J = 15 Hz), 106.9, 105.1 (t, J = 30 Hz), 63.7, 29.5, 25.1, 22.5, 21.4, 8.5, 4.8 (2C); HRMS for $\text{C}_{23}\text{H}_{23}\text{F}_2\text{N}_7\text{O}_3$ ($\text{M} + \text{H}$) $^+$ calcd 484.1908, found 484.1904.

5-(6-(5-(Difluoromethyl)-1,3,4-oxadiazol-2-yl)-5-isopropylpyrrolo[2,1-f][1,2,4]triazin-4-ylamino)-2,4-difluoro-N-methoxybenzamide (44): off-white solid; Anal. RP-HPLC t_R = 3.78 min (column B, purity 98%); ^1H NMR (400 MHz, CD_3OD) δ 8.13 (s, 1H), 7.73–7.68 (m, 1H), 7.59 (s, 1H), 7.23 (t, 1H, J = 10.4 Hz), 7.13 (t, 1H, J = 50 Hz), 4.11–4.05 (m, 1H), 3.73 (s, 3H), 1.42 (d, 6H, J = 7.1 Hz); ^{13}C NMR (100 MHz, $\text{DMSO}-d_6$) δ 162.9, 160.7, 157.7, 155.8 (dd, J = 251, 14 Hz), 155.1 (dd, J = 251, 14 Hz), 141.4, 139.5, 131.9 (d, J = 15 Hz), 130.5, 124.6, 122.4, 118.6 (d, J = 15 Hz), 116.7, 107.0 (t, J = 238 Hz), 106.0 (t, J = 30 Hz), 105.5, 63.7, 25.2, 21.3, 21.1; HRMS for $\text{C}_{20}\text{H}_{17}\text{F}_4\text{N}_7\text{O}_3$ ($\text{M} + \text{H}$) $^+$ calcd 480.1407, found 480.1410. Anal. ($\text{C}_{20}\text{H}_{17}\text{F}_4\text{N}_7\text{O}_3$) C, H, N.

2,4-Difluoro-5-(5-isopropyl-6-(5-(trifluoromethyl)-1,3,4-oxadiazol-2-yl)-pyrrolo[2,1-f][1,2,4]triazin-4-ylamino)-N-methoxybenzamide (45): off-white solid; Anal. RP-HPLC t_R = 3.81 min (column B, purity 98%); ^1H NMR (400 MHz, CD_3OD) δ 8.09 (s, 1H), 7.71–7.67 (m, 1H), 7.56 (s, 1H), 7.24 (t, 1H, J = 10.1 Hz), 4.35 (hep, 1H, J = 7.2 Hz), 3.80 (s, 3H), 1.51 (d, 6H, J = 7.2 Hz); ^{13}C NMR (100 MHz, $\text{DMSO}-d_6$) δ 163.7, 160.5, 160.1, 156.0 (dd, J = 255, 17 Hz), 155.6 (dd, J = 255, 17 Hz), 153.5, 153.1, 143.3, 130.5, 122.8, 122.2, 118.6 (d, J = 20 Hz), 118.0 (q, J = 274 Hz), 116.7, 116.3, 106.0 (t, J = 28 Hz), 63.7, 25.3, 21.3 (2C); HRMS for $\text{C}_{20}\text{H}_{16}\text{F}_5\text{N}_7\text{O}_3$ ($\text{M} + \text{H}$) $^+$ calcd 498.1313, found 498.1297.

2,4-Difluoro-5-(5-isopropyl-6-(5-(2,2,2-trifluoroethyl)-1,3,4-oxadiazol-2-yl)pyrrolo[2,1-f][1,2,4]triazin-4-ylamino)-N-methoxybenzamide (46): pale yellow oil; Anal. RP-HPLC t_R = 1.71 min (column A, purity 99%); ^1H NMR (400 MHz, CDCl_3) δ 9.17–9.14 (m, 2H), 8.03–7.97 (m, 2H), 7.45 (bs, 1H), 7.00 (t, 1H, J = 10.3 Hz), 4.19–4.14 (m, 1H), 3.86 (s, 3H), 3.79 (q, 2H, J = 9.6 Hz), 1.50 (d, 6H, J = 7.2 Hz); MS (ESI) m/z 512 ($\text{M} + \text{H}$) $^+$.

5-(6-(5-(Dimethylamino)methyl)-1,3,4-oxadiazol-2-yl)-5-isopropylpyrrolo[2,1-f][1,2,4]triazin-4-ylamino)-2,4-difluoro-N-methoxybenzamide, Trifluoroacetic Acid Salt (48): pale yellow oil; Anal. RP-HPLC t_R = 1.23 min (column A, purity 90%); ^1H NMR (400 MHz, CD_3OD) δ 8.01 (s, 1H),

7.72–7.48 (m, 2H), 7.22 (t, 1H, J = 10.3 Hz), 4.82 (s, 2H), 4.37–4.28 (m, 1H), 3.82 (s, 3H), 3.31 (s, 3H), 3.11 (s, 3H), 1.51 (d, 6H, J = 7.1 Hz); MS (ESI) m/z 487 ($\text{M} + \text{H}$) $^+$.

2,4-Difluoro-5-(5-isopropyl-6-(5-(methylsulfonylmethyl)-1,3,4-oxadiazol-2-yl)pyrrolo[2,1-f][1,2,4]triazin-4-ylamino)-N-methoxybenzamide (49): white solid; Anal. RP-HPLC t_R = 2.75 min (column B, purity 96%); ^1H NMR (400 MHz, CD_3OD) δ 8.03 (s, 1H), 7.73–7.66 (m, 1H), 7.52 (s, 1H), 7.16 (t, 1H, J = 10.0 Hz), 4.83 (s, 2H), 3.93 (hep, 1H, J = 7.0 Hz), 3.67 (s, 3H), 3.04 (s, 3H), 1.34 (d, 6H, J = 7.0 Hz); HRMS for $\text{C}_{21}\text{H}_{21}\text{F}_2\text{N}_7\text{O}_5\text{S}$ ($\text{M} + \text{H}$) $^+$ calcd 522.1371, found 522.1369.

2,4-Difluoro-5-(5-isopropyl-6-(1,3,4-oxadiazol-2-yl)pyrrolo[2,1-f][1,2,4]triazin-4-ylamino)-N-methoxybenzamide (38): A solution of hydrazide **35** (48 mg, 0.20 mmol) and triethyl orthoformate (0.2 mL) in EtOH (2 mL) was heated to 120 °C for 7 h. The reaction mixture was cooled to room temperature, and the volatiles were removed under reduced pressure. The residue was triturated with Et₂O to give 5-isopropyl-6-(1,3,4-oxadiazol-2-yl)pyrrolo[2,1-f][1,2,4]triazin-4(3H)-one (10 mg, 0.041 mmol, 20%), which was used directly in the next step without further purification; Anal. RP-HPLC t_R = 1.23 min (column A, purity 98%); ^1H NMR (400 MHz, $\text{DMSO}-d_6$) δ 11.8 (bs, 1H), 8.15 (s, 1H), 8.04 (s, 1H), 7.92 (s, 1H), 4.18 (hep, 1H, J = 7.2 Hz), 2.50 (s, 3H), 1.37 (d, 6H, J = 7.2 Hz); MS (ESI) m/z 246 ($\text{M} + \text{H}$) $^+$.

The 5-isopropyl-6-(1,3,4-oxadiazol-2-yl)pyrrolo[2,1-f][1,2,4]triazin-4(3H)-one (10 mg, 0.041 mmol) was dissolved in POCl_3 (1 mL) and the reaction mixture was stirred at 120 °C for 5 h. The excess POCl_3 was removed under reduced pressure and the residue was coevaporated with toluene. The residue was dissolved in MeCN and treated with 5-amino-2,4-difluoro-N-methoxybenzamide (8.3 mg, 0.041 mmol). The reaction mixture was stirred at room temperature for 19 h, the solvent was removed under reduced pressure, and the residue was purified by preparative HPLC to afford **38** (9.8 mg, 56%) as a white solid; Anal. RP-HPLC t_R = 1.43 min (column A, purity 98%); ^1H NMR (400 MHz, CD_3OD) δ 9.00 (s, 1H), 8.01 (s, 1H), 7.71–7.67 (m, 1H), 7.57 (s, 1H), 7.25 (t, 1H, J = 10.1 Hz), 4.33–4.27 (m, 1H), 3.85 (s, 3H), 1.50 (d, 6H, J = 7.1 Hz); HRMS for $\text{C}_{19}\text{H}_{17}\text{F}_2\text{N}_7\text{O}_3$ ($\text{M} + \text{H}$) $^+$ calcd 430.1394, found 430.1399.

5-(6-(5-(Dimethylamino)-1,3,4-oxadiazol-2-yl)-5-isopropylpyrrolo[2,1-f][1,2,4]triazin-4-ylamino)-2,4-difluoro-N-methoxybenzamide (47): A solution of hydrazide **35** (92 mg, 0.39 mmol) and phosgene iminium chloride (76 mg, 0.47 mmol) in MeCN was heated to 80 °C for 6 h. The reaction mixture was cooled to room temperature and diluted with water (4 mL). The precipitate that formed after 5 min of stirring was filtered, washed with water, and dried overnight to give 6-(5-(dimethylamino)-1,3,4-oxadiazol-2-yl)-5-isopropylpyrrolo[2,1-f][1,2,4]triazin-4(3H)-one (91 mg, 0.32 mmol, 82%) as a colorless oil; Anal. RP-HPLC t_R = 1.35 min (column A, purity 97%); ^1H NMR (400 MHz, CD_3OD) δ 7.79 (s, 1H), 7.48 (s, 1H), 3.92 (hep, 1H, J = 7.2 Hz), 3.07 (s, 3H), 3.05 (s, 3H), 1.27 (d, 6H, J = 7.2 Hz); MS (ESI) m/z 289 ($\text{M} + \text{H}$) $^+$.

A mixture of 6-(5-(dimethylamino)-1,3,4-oxadiazol-2-yl)-5-isopropylpyrrolo[2,1-f][1,2,4]triazin-4(3H)-one (91 mg, 0.32 mmol) in POCl_3 (3 mL) was heated to 120 °C for 5 h. The excess POCl_3 was removed under reduced pressure and the residue was coevaporated with toluene. The residue was dissolved in MeCN (5 mL) and treated with 5-amino-2,4-difluoro-N-methoxybenzamide (63 mg, 0.31 mmol). The reaction mixture was stirred at room temperature for 16 h, the solvent was removed under reduced pressure, and the residue was purified by preparative HPLC to afford **47** (81 mg, 55%) as an off white solid; Anal. RP-HPLC t_R = 1.50 min (column A, purity 99%); ^1H NMR (400 MHz, CD_3OD) δ 7.78 (s, 1H), 7.59–7.55 (m, 1H), 7.39 (m, 1H), 7.07 (t, 1H, J = 10.1 Hz), 4.09–4.01 (m, 1H), 3.68 (s, 3H), 3.06 (s, 6H), 1.32 (d, 6H, J = 7.1 Hz); HRMS for $\text{C}_{21}\text{H}_{22}\text{F}_2\text{N}_8\text{O}_3$ ($\text{M} + \text{H}$) $^+$ calcd 473.1805, found 473.1810.

5-(6-(5-(Difluoro(methylsulfonyl)methyl)-1,3,4-oxadiazol-2-yl)-5-isopropylpyrrolo[2,1-f][1,2,4]triazin-4-ylamino)-2,4-difluoro-N-methoxybenzamide (50): To a solution of **49** (0.89 g, 1.7 mmol) in THF (100 mL) at –78 °C was slowly added 1 N lithium bis(trimethylsilyl)amide in THF (6.9 mL,

6.9 mmol). The reaction mixture was stirred for 10 min at -78°C and then warmed to -40°C . A solution of *N*-fluorobenzene sulfonamide (1.4 g, 4.3 mmol) in THF (10 mL) was added dropwise to the reaction mixture and the resulting solution was stirred for 1 h at -30 to -40°C . The reaction was quenched by the addition of cold saturated aqueous NH_4Cl solution (100 mL), and the mixture was extracted with EtOAc (3×100 mL). The EtOAc portions were dried (Na_2SO_4) and concentrated in vacuo, and the residue was purified by flash chromatography (SiO_2 , 0–2% MeOH/ CH_2Cl_2 gradient elution) to give **50** (0.63 g, 65%) as a white solid: Anal. RP-HPLC $t_{\text{R}} = 3.33$ min (column B, purity 97%); ^1H NMR (400 MHz, CDCl_3) δ 9.09–9.03 (m, 2H), 8.04 (s, 1H), 7.93 (s, 1H), 7.50 (bs, 1H), 6.91 (t, 1H, $J = 10.3$ Hz), 4.08–4.01 (m, 1H), 3.78 (s, 3H), 3.16 (s, 3H), 1.43 (d, 6H, $J = 7.0$ Hz); ^{13}C NMR (100 MHz, CDCl_3 with one drop CD_3OD) δ 164.4, 161.2, 155.6 (dd, $J = 256$, 14 Hz), 154.9 (dd, $J = 256$, 14 Hz), 153.2 (t, $J = 30$ Hz), 133.0, 127.5, 126.0 (2C), 121.5, 116.2, 116.1, 113.8 (t, $J = 288$ Hz), 105.4, 104.6 (t, $J = 28$ Hz), 63.6, 35.3, 25.5, 21.0 (2C); HRMS for $\text{C}_{21}\text{H}_{19}\text{F}_4\text{N}_7\text{O}_5\text{S}$ ($\text{M} + \text{H}$) $^+$ calcd 558.1165, found 558.1163. Anal. ($\text{C}_{21}\text{H}_{19}\text{F}_4\text{N}_7\text{O}_5\text{S}$) C, H, N.

2,4-Difluoro-5-(5-isopropyl-6-(5-methyl-4H-1,2,4-triazol-3-yl)pyrrolol[2,1-f][1,2,4]triazin-4-ylamino)-N-methoxybenzamide, Hydrochloride Salt (52). A mixture of **35** (24 mg, 0.10 mmol) and acetamide hydrochloride (14 mg, 0.15 mmol) in DMF (1 mL) was heated at 120°C for 1 h. The reaction mixture was diluted with MeOH and purified by preparative HPLC to give **51** (22 mg, 0.086 mmol, 86%) as a white solid: Anal. RP-HPLC $t_{\text{R}} = 1.71$ min (column B, purity 97%); ^1H NMR (400 MHz, $\text{DMSO}-d_6$) δ 8.18 (s, 1H), 7.90 (s, 1H), 4.21 (hep, 1H, $J = 7.2$ Hz), 2.40 (s, 3H), 1.35 (d, 6H, $J = 7.1$ Hz); MS (ESI) m/z 259 ($\text{M} + \text{H}$) $^+$.

The triazole **51** (22 mg, 0.086 mmol) was treated with POCl_3 (1 mL) and the reaction mixture was stirred at 120°C for 5 h. The excess POCl_3 was removed under reduced pressure and the residue was coevaporated with toluene. The residue was dissolved in 2-propanol and stirred with *N*-methoxyl-5-amino-2,4-difluorobenzamide (20 mg, 0.10 mmol) at 50°C for 1 h. The solvent was removed in vacuo and the residue was purified by preparative HPLC. The product was converted to the hydrochloride salt by treatment with aqueous 1 N HCl followed by lyophilization to afford **52** (27 mg, 71%) as a white solid: Anal. RP-HPLC $t_{\text{R}} = 3.17$ min (column B, purity 98%); ^1H NMR (400 MHz, CD_3OD) δ 7.88 (s, 1H), 7.69–7.63 (m, 1H), 7.56 (s, 1H), 7.22 (t, 1H, $J = 10.2$ Hz), 4.10 (hep, 1H, $J = 7.2$ Hz), 3.82 (s, 3H), 2.74 (s, 3H), 1.43 (d, 6H, $J = 7.2$ Hz); HRMS for $\text{C}_{20}\text{H}_{20}\text{F}_2\text{N}_8\text{O}_2$ ($\text{M} + \text{H}$) $^+$ calcd 443.1742, found 443.1748.

In Vitro Kinase Assays. The enzyme inhibition studies were carried out as previously described.²³ Recombinant proteins containing either the cytoplasmic domains of the human receptor tyrosine kinases (VEGFR-2, Flk-1, FGFR-1, PDGFR- β , IGF-1R, HER-1, HER-2) or the entire protein sequence for the serine/threonine kinases (PKC and CDK2) were expressed as *n*-terminal glutathione *S*-transferase (GST) fusion proteins using the baculovirus expression vector system in Sf9 cells. The resultant proteins were isolated by affinity chromatography using glutathione-Sepharose (Pharmacia Biotech). All enzymes were stored at -80°C . The kinase assays were performed in 96-well microtiter plates using the synthetic polymer poly(Glu₄/Tyr) (Sigma Chemicals) as a phosphoacceptor substrate. TCA precipitates were collected onto GF/C unfilter plates (Packard Instrument Co., Meriden, CT) using a Filtermate universal harvester (Packard Instrument Co.), and the filters were quantitated using a TopCount 96-well liquid scintillation counter (Perkin-Elmer Life Sciences). Procedures for assessing activity of the representative nonreceptor tyrosine kinase Lck and the serine-threonine kinases PKC α and CDK2 have been previously described.^{34,35}

For the VEGFR-2, Flk-1, FGFR-1, and PDGFR- β kinase assays, compounds were dissolved in DMSO and diluted with water/10% DMSO to a final DMSO concentration of 2%. The VEGFR-2 kinase reactions consisted of 8 ng of GST-VEGFR-2 enzyme, 75 $\mu\text{g}/\text{mL}$ substrate, 1 μM ATP, and 0.04 μCi [γ - ^{33}P]-ATP in 50 μL total reaction volume (kinase buffer: 20 mM

Tris, pH 7.0, 25 $\mu\text{g}/\text{mL}$ BSA, 1.5 mM MnCl_2 , 0.5 mM dithiothreitol). The Flk-1 kinase reactions consisted of 10 ng of GST-Flk-1 enzyme, 75 $\mu\text{g}/\text{mL}$ substrate, 1 μM ATP, and 0.04 μCi [γ - ^{33}P]-ATP in 50 μL total reaction volume (kinase buffer: 20 mM Tris, pH 7.0, 25 $\mu\text{g}/\text{mL}$ BSA, 4 mM MnCl_2 , 0.5 mM dithiothreitol). The FGFR-1 kinase reactions consisted of 10 ng of GST-FGFR-1 enzyme, 75 $\mu\text{g}/\text{mL}$ substrate, 1 μM ATP, and 0.04 μCi [γ - ^{33}P]-ATP in 50 μL total reaction volume (kinase buffer: 20 mM Tris, pH 7.0, 25 $\mu\text{g}/\text{mL}$ BSA, 0.5 mM MnCl_2 , 0.5 mM MgCl_2 , and 0.5 mM dithiothreitol). The PDGFR- β kinase reactions consisted of 10 ng GST-PDGFR- β enzyme, 180 $\mu\text{g}/\text{mL}$ substrate, 1 μM ATP, and 0.04 μCi [γ - ^{33}P]-ATP in 50 μL total reaction volume (kinase buffer: 16 mM HEPES, pH 7.0, 80 $\mu\text{g}/\text{mL}$ BSA, 4 mM MnCl_2 , 120 mM NaCl, and 0.5 mM dithiothreitol). In all cases, the reactions were incubated for 60 min at 27°C and terminated with the addition of cold trichloroacetic acid (TCA) to a final concentration of 15%.

For the IGF-1R kinase assay, reactions consisted of 125 ng of GST-IGF-1R enzyme, 25 ng substrate, and 25 μM of [γ - ^{33}P]-ATP in a final reaction volume of 50 μL (kinase buffer: 20 mM MOPS, pH 7.0, 0.1 mg/mL BSA, 5 mM MnCl_2 , and 0.1 mM dithiothreitol). The reactions were incubated at 27°C for 60 min.

For HER-2, the entire cytoplasmic sequence was expressed without an affinity tag. The protein was partially purified by ion-exchange chromatography on DEAE-Sepharose (Pharmacia Biotech) and was eluted with a buffer containing 0.3 M NaCl. For both the HER-1 and HER-2 kinase assays, the reactions consisted of 10 ng of GST-HER-1 or 150 ng of partially purified HER-2 enzyme, 1.5 μM substrate, 1 μM ATP, and 0.15 μCi [γ - ^{33}P]-ATP in a total reaction volume of 50 μL (kinase buffer: 50 mM Tris-HCl pH 7.7, 0.1 mg/mL BSA, 10 mM MnCl_2 , and 2 mM dithiothreitol). The reactions were incubated at 27°C for 60 min and terminated by the addition of 10 μL of stop buffer (2.5 mg/mL BSA and 0.3 M EDTA), followed by 108 μL of a mixture of 3.5 mM ATP and 5% TCA. The percent inhibition from the kinase assays was determined by nonlinear regression analyses, and data were reported as the inhibitory concentration required to achieve 50% inhibition relative to control reactions (IC_{50}).

The apparent K_i value for **50** was determined by global fitting of background-corrected cpm data to a competitive model versus ATP using GraFit software, version 5 (Erihtacus Software Ltd).

Cellular Proliferation Assays. Primary human umbilical vein endothelial cells (HUVECs) were purchased from Clonetics (catalog # CC-2519) and not used beyond passage 3 for the mitogen-stimulated proliferation assays as previously described.²³ The concentrations of VEGF (Peprotech) and FGF (Clonetics) used in the mitogen-stimulated HUVEC assays were 8 and 80 ng/mL, respectively. The L2987 human lung carcinoma cells were not used beyond passage 20 for serum-stimulated proliferation assays. For compound assessment, cells were grown in 100 μL of minimal growth medium (Cellgro catalog # 10–040-CV) and 1.0% heat-inactivated fetal bovine serum (Cellgro catalog # 10–040-CV) in 96-well collagen IV coated plates (Bectin-Dickinson, catalog # 354429) at a density of 2×10^3 per well in a $37^{\circ}\text{C}/5\%$ CO_2 environment. Twenty-four hours later, serum was adjusted to 10%, and test compounds at various dilutions were added to each well in a final volume of minimal growth media that contains 10% serum. Forty-eight hours later, 0.5 μCi of [^3H]thymidine (Amersham catalog # TRK120) was added in a volume of 20 μL of minimal media for 24 h. Plates were washed once in PBS. Upon removal of PBS, Trypsin (Cellgro catalog numbers 21-031-CV and 25-054-CI, respectively) was added to cells which were subsequently harvested onto glass-fiber filters (Perkin-Elmer-Life-Sciences catalog # 1450–525) using an automated harvester (Brandel Model# MWX RI-192TI). Incorporated tritium was quantified using a β -counter (Wallac Microbeta). Dose–response curves were generated to determine the IC_{50} value, which is defined as the concentration of drug required to inhibit 50% of tritium incorporation when compared to untreated serum-stimulated cells.

Metabolic Stability. The compound was incubated with human liver microsomes purchased from In Vitro Technologies (Baltimore, MD) and pooled from 10 individual donors. The rates of oxidative metabolism were measured under the following conditions: compound (substrate) at 3 or 10 μM final concentration, final microsomal protein concentration of approximately 1 mg/mL, 1 mM NADPH, and 56 mM of pH 7.4 potassium phosphate buffer. Incubations were performed at 37 °C and were initiated by the addition of the substrate. Incubations were quenched by the addition of one volume of acetonitrile after 10 min. Samples were then analyzed for the parent compound by LC-MS. The rate of metabolism was calculated by determining the nanomoles of parent compound oxidized and dividing it by the time of incubation and the milligrams of protein.

Cytochrome P450 Assay. The ability of compounds to inhibit the major human cytochrome P450s (CYPs) responsible for drug metabolism was evaluated in vitro using recombinant human CYP isoforms. The inhibition of cDNA-derived CYP enzymes prepared from baculovirus-infected insect cells was measured using either 3-cyano-7-ethoxycoumarin (CYP1A2, CYP2C19), 7-methoxy-4-trifluoromethylcoumarin (CYP2C9), or 3-[2-(*N,N*-diethyl-*N*-methylamino)ethyl]-7-methoxy-4-methylcoumarin (CYP2D6) as the substrates. CYP3A4 inhibition was evaluated with two substrates: 7-benzyloxy-4-trifluoromethylcoumarin (BFC) and resorufin benzyl ether (BzRes). A single concentration of each model substrate (at approximately the apparent K_m , with the exception of BFC, which was tested below the apparent K_m) and multiple concentrations of the test compounds, separated by approximately 1/2 log units, were tested in duplicate. Metabolism of the model substrates was assayed by the production of 7-hydroxy-3-cyanocoumarin, 3-[2-(*N,N*-diethylamino)ethyl]-7-hydroxy-4-methylcoumarin, 7-hydroxy-4-trifluoromethylcoumarin, or resorufin and measured via fluorescence detection. Assays were conducted in 96-well microtiter plates in the presence of an NADPH-generating system. Positive control samples were included in these studies. The positive control values were within the historical range for all the assays. The IC_{50} values were calculated utilizing XLfit curve-fitting software.

Pharmacokinetic Parameters Obtained in Mice. In these 4 h oral exposure studies, a single-dose of 50 mg/kg of compounds **24–26**, **37**, **44**, **49**, and **50** (10 mg/kg) was delivered as a solution in 70% PEG400/10% ethanol/20% water by oral gavage to fasted adult male Balb/C mice ($n = 3$ per compound). Three serum samples were collected from each mouse at 0.5, 1, and 4 h time points following oral dosing. The first two samples were obtained by retro-orbital bleed ($\sim 100 \mu\text{L}$ /20–25 g mouse) and the third sample by cardiac puncture. The blood samples were allowed to clot on ice and centrifuged and then the serum was harvested. Plasma samples were stored at $-20 \text{ }^\circ\text{C}$ prior to analysis. The plasma samples were analyzed for parent compound via HPLC-coupled tandem mass spectrometry (LC-MS/MS).

To evaluate the oral bioavailability of compound **50** in male Balb/C mice, a single dose was delivered as a solution in 30% PEG 400/10% ethanol/60% water by either tail vein injection (iv, 5 mg/kg) or by oral gavage (po, 10 mg/kg). The mice were fasted overnight prior to dosing and fed 4 h post dose. A total of 18 mice were used in the study ($n = 9$ each for iv and po groups). Three serum samples were collected from each mouse, the first two samples by retro-orbital bleed ($\sim 100 \mu\text{L}$ /20–25 g mouse) and the third sample by cardiac puncture. Blood samples were collected at 0.5, 0.5, 1, 3, 6, 8, 10, 12, and 24 h time points following iv dosing and at 0.25, 0.5, 1, 3, 6, 8, 10, 12, and 24 h following oral dosing. Blood samples were allowed to clot on ice and centrifuged, and then serum was harvested. Plasma samples were stored at $-20 \text{ }^\circ\text{C}$ until analysis. Concentrations of parent compound were later determined by LC-MS/MS. Composite serum concentration-time profiles were constructed for pharmacokinetic analysis.

Serum Protein Binding of Compound 50. The extent of protein binding of compound **50** was determined in mouse and human sera using the equilibrium dialysis method. All experiments were carried out using pooled serum ($n = 10$ for

mice, $n = 3$ for human) obtained from Bioreclamation Inc. (Hicksville, NY). Compound **50** (1 mM) in acetonitrile was added to serum at a ratio of 1:100 to give a final concentration of 10 μM . Serum samples were dialyzed against 134 mM phosphate buffer (pH 7.4). The Micro-Equilibrium Dialyzer (500 μL chamber volume, Amika Corp., Holliston, MA) containing spiked serum was incubated in a shaking water bath maintained at 37 °C for 4 h. A 10 000 molecular weight cutoff dialysis membrane (Amika Corp., Holliston, MA) was used. All experiments were carried out in triplicate. Aliquots of buffer and serum were taken at 4 h, and analyzed by LC-MS/MS. Compound **50** was stable under these conditions over the 4 h incubation period in mouse and human serum.

From each dialysis cell, the free and bound drug percentages were calculated as follows:

$$\begin{aligned} \% \text{ free} &= 100 \times (\text{concentration in buffer}) / \\ &\quad (\text{concentration in serum}) \\ \% \text{ bound} &= 100 - \% \text{ free} \end{aligned}$$

In Vivo Antitumor Activity in the Subcutaneously Implanted L2987 Xenograft Model in Nude Mice. Female Balb/C athymic (nu+/nu+) mice, 6–8 weeks old, were obtained from Sprague-Dawley Co. (Indianapolis, IN). Animals were provided with food and water ad libitum and housed five per cage. Mice were maintained in accordance with Bristol-Myers Squibb's Institutional Animal Care and Use Committee in accordance with the American Association for Accreditation of Laboratory Animal Care (AAALAC) guidelines for the humane treatment and care of laboratory mice.

L2987 tumor fragments⁴² maintained by serial passage in vivo were implanted subcutaneously in the hind flank using an 18 g trocar. Approximately 2 weeks postimplant, when tumor sizes reached 100–150 mm³, oral dosing was initiated using gavage needles with either compound at the indicated concentrations or vehicle (7:1:2 PEG400/EtOH/H₂O) in the control group. Tumor growth was assessed twice weekly by vernier caliper measurement. Group sizes were $n = 8$ or 9.

Treatments resulting in greater than 20% lethality and/or 20% body weight loss were considered toxic. Antitumor activity was determined by calculating the maximum percent tumor growth inhibition (TGI) of treated animals at the indicated time points using the formula

$$\% \text{TGI} = \{(C_t - T_t)/(C_t - C_0)\} \times 100$$

where C_t = the median tumor volume (mm³) of vehicle-treated control (C) mice at time t . T_t = median tumor volume of treated (T) mice at time t . C_0 is the median tumor volume of control mice at time 0. Activity is defined as a continuous %TGI > 50% for at least one tumor volume doubling time after the start of drug treatment.

Acknowledgment. The authors wish to thank John Hynes for his seminal contributions on the hydroxamate-based pyrrolo[2,1-*f*][1,2,4]triazines; Amy Camuso, Steven Dzwonczyk, Kurt Gregor, Stephanie Kut, Aixin Li, and Chiang Yu for conducting the kinase selectivity assays; Hilary Gray for protein expression and purification; Mark Witmer for assistance with the enzyme kinetics; Victor Cardenas for informatics support; Brian Fink for helpful discussions; and the Discovery Analytical Sciences Department for obtaining high-resolution MS analyses.

Supporting Information Available: A general procedure for the synthesis of the C6-carbamate library, a table of pertinent data for the C6-carbamate analogues, and a table of combustion analysis or HPLC analysis data for key compounds. This material is available free of charge via the Internet at <http://pubs.acs.org>.

References

- (1) (a) Folkman, J.; Shing, Y. *Angiogenesis*. *J. Biol. Chem.* **1992**, *267*, 10931–10934. (b) Griffioen, A. W.; Molema, G. *Angiogenesis: Potentials for pharmacologic intervention in the treatment of cancer, cardiovascular diseases, and chronic inflammation*. *Pharmacol. Rev.* **2000**, *52*, 237–268.
- (2) Folkman, J.; Klagsbrun, M. *Angiogenic factors*. *Science* **1987**, *235*, 442–447.
- (3) (a) Folkman, J. *Angiogenesis in cancer, vascular, rheumatoid and other diseases*. *Nat. Med.* **1995**, *1*, 27–31. (b) Carmeliet, P.; Jain, R. K. *Angiogenesis in cancer and other diseases*. *Nature* **2000**, *407*, 249–257. (c) Folkman, J. *Angiogenesis-dependent diseases*. *Semin. Oncol.* **2001**, *28*, 536–542. (d) Fan, T.-P. D.; Jaggar, R.; Bicknell, R. *Controlling the vasculature: Angiogenesis, anti-angiogenesis and vascular targeting gene therapy*. *Trends Pharm. Sci.* **1995**, *16*, 57–66.
- (4) (a) Koch, A. E. *Angiogenesis as a target in rheumatoid arthritis*. *Ann. Rheum. Dis.* **2003**, *62*, ii60–ii67. (b) Walsh, D. A. *Angiogenesis and arthritis*. *Rheumatol.* **1999**, *38*, 103–112. (c) Koch, A. E. *Angiogenesis: Implications for rheumatoid arthritis*. *Arthritis Rheum.* **1998**, *41*, 951–962.
- (5) (a) Folkman, J. *Anti-angiogenesis: New concept for therapy of solid tumors*. *Ann. Surg.* **1972**, *175*, 409–416. (b) Folkman, J. *What is the evidence that tumors are angiogenesis dependent?* *J. Natl. Cancer Inst.* **1990**, *83*, 4–6.
- (6) (a) Thomas, K. A. *Vascular endothelial growth factor, a potent and selective angiogenic agent*. *J. Biol. Chem.* **1996**, *271*, 603–606. (b) Ferrara, N.; Davis-Smyth, T. *The biology of vascular endothelial growth factor*. *Endocr. Rev.* **1997**, *18*, 4–25. (c) Ferrara, N. *VEGF: An update on biological and therapeutic aspects*. *Curr. Opin. Biotech.* **2000**, *11*, 617–624.
- (7) Traxler, P. *Tyrosine kinases as targets in cancer therapy—Successes and failures*. *Exp. Opin. Ther. Targets* **2003**, *7*, 215–234.
- (8) Shawver, L. K.; Lipson, K. E.; Fong, T. A. T.; McMahon, G.; Plowman, G. D.; Strawn, L. M. *Receptor tyrosine kinases as targets for inhibition of angiogenesis*. *Drug Discov. Today* **1997**, *2*, 50–63.
- (9) (a) Caponigro, F. *Rationale and clinical validation of epidermal growth factor receptor as a target in the treatment of head and neck cancer*. *Anti-Cancer Drugs* **2004**, *15*, 311–320. (b) Tiseo, M.; Loprevite, M.; Ardizzoni, A. *Epidermal growth factor receptor inhibitors: A new prospective in the treatment of lung cancer*. *Curr. Med. Chem.: Anti-Cancer Agents* **2004**, *4*, 139–148.
- (10) (a) Zondor, S. D.; Medina, P. J. *Bevacizumab: An angiogenesis inhibitor with efficacy in colorectal and other malignancies*. *Annals of Pharmacotherapy* **2004**, *38*, 1258–1264. (b) Ferrara, N.; Hillan, K. J.; Gerber, H.-P.; Novotny, W. *Discovery and development of bevacizumab, an anti-VEGF antibody for treating cancer*. *Nat. Rev. Drug Disc.* **2004**, *3*, 391–400. (c) Hurwitz, H.; Fehrenbacher, L.; Novotny, W.; Cartwright, T.; Hainsworth, J.; Heim, W.; Berlin, J.; Baron, A.; Griffing, S.; Holmgren, E.; Ferrara, N.; Fyfe, G.; Rogers, B.; Ross, R.; Kabbinavar, F. *Bevacizumab plus irinotecan, fluorouracil, and leucovorin for metastatic colorectal cancer*. *New Engl. J. Med.* **2004**, *350*, 2335–2342.
- (11) (a) Underiner, T. L.; Ruggeri, B.; Gingrich, D. E. *Development of vascular endothelial growth factor receptor (VEGFR) kinase inhibitors as anti-angiogenic agents in cancer therapy*. *Curr. Med. Chem.* **2004**, *11*, 731–745. (b) Bilodeau, M. T.; Fraley, M. E.; Hartman, G. D. *Kinase insert domain-containing receptor kinase inhibitors as anti-angiogenic agents*. *Exp. Opin. Invest. Drugs* **2002**, *11*, 737–745. (c) Sepp-Lorenzino, L.; Thomas, K. A. *Antiangiogenic agents targeting vascular endothelial growth factor and its receptors in clinical development*. *Exp. Opin. Investig. Drugs* **2002**, *11*, 1447–1465.
- (12) (a) Wood, J. M.; Bold, G.; Buchdunger, E.; Cozens, R.; Ferrari, S.; Frei, J.; Hofmann, F.; Mestan, J.; Mett, H.; O'Reilly, T.; Persohn, E.; Rösler, J.; Schnell, C.; Stover, D.; Theuer, A.; Towbin, H.; Wenger, F.; Woods-Cook, K.; Menrad, A.; Siemeister, G.; Schirner, M.; Thierauch, K.-H.; Schneider, M. R.; Drevs, J.; Martiny-Baron, G.; Totzke, F.; Marmé, D. *PTK787/ZK 222584, a novel and potent inhibitor of vascular endothelial growth factor receptor tyrosine kinases, impairs vascular endothelial growth factor-induced responses and tumor growth after oral administration*. *Cancer Res.* **2000**, *60*, 2178–2189. (b) Bold, G.; Altmann, K.-H.; Frei, J.; Lang, M.; Manley, P. W.; Traxler, P.; Wietfeld, B.; Brügggen, J.; Buchdunger, E.; Cozens, R.; Ferrari, S.; Furet, P.; Hofmann, F.; Martiny-Baron, G.; Mestan, J.; Rösler, J.; Sills, M.; Stover, D.; Acemoglu, F.; Boss, E.; Emmenegger, R.; Lässer, L.; Masso, E.; Roth, R.; Schlachter, C.; Vetterli, W.; Wyss, D.; Wood, J. M. *New anilinothalazines as potent and orally well absorbed inhibitors of the VEGF receptor tyrosine kinases useful as antagonists of tumor-driven angiogenesis*. *J. Med. Chem.* **2000**, *43*, 2310–2323. (c) Furet, P.; Bold, G.; Hofmann, F.; Manley, P.; Meyer, T.; Altmann, K.-H. *Identification of a new chemical class of potent angiogenesis inhibitors based on conformational considerations and database searching*. *Bioorg. Med. Chem. Lett.* **2003**, *13*, 2967–2971. (d) Manley, P. W.; Furet, P.; Bold, G.; Brügggen, J.; Mestan, J.; Meyer, T.; Schnell, C. R.; Wood, J.; Haberey, M.; Huth, A.; Krüger, M.; Menrad, A.; Ottow, E.; Seidelmann, D.; Siemeister, G.; Thierauch, K.-H. *Anthranilic acid amides: A novel class of antiangiogenic VEGF receptor kinase inhibitors*. *J. Med. Chem.* **2002**, *45*, 5687–5693.
- (13) (a) Sun, L.; Liang, C.; Shirazian, S.; Zhou, Y.; Miller, T.; Cui, J.; Fukuda, J. Y.; Chu, J.-Y.; Nematalla, A.; Wang, X.; Chen, H.; Sistla, A.; Luu, T. C.; Tang, F.; Wei, J.; Tang, C. *Discovery of 5-[5-fluoro-2-oxo-1,2-dihydroindol-(3Z)-ylidene-methyl]-2,4-dimethyl-1H-pyrrole-3-carboxylic acid (2-diethylaminoethyl)amide, a novel tyrosine kinase inhibitor targeting vascular endothelial and platelet-derived growth factor receptor tyrosine kinase*. *J. Med. Chem.* **2003**, *46*, 1116–1119. (b) Abrams, T. J.; Murray, L. J.; Pesenti, E.; Walker Holway, V.; Colombo, T.; Lee, L. B.; Cherrington, J. M.; Pryer, N. K. *Preclinical evaluation of the tyrosine kinase inhibitor SU11248 as a single agent and in combination with “standard of care” therapeutic agents for the treatment of breast cancer*. *Mol. Cancer Ther.* **2003**, *2*, 1011–1021. (c) Sun, L.; Tran, N.; Liang, C.; Hubbard, S.; Tang, F.; Lipson, K.; Schreck, R.; Zhou, Y.; McMahon, G.; Tang, C. *Identification of substituted 3-[(4,5,6,7-tetrahydro-1H-indol-2-yl)methylene]-1,3-dihydroindol-2-ones as growth factor receptor inhibitors for VEGF-R2 (Flk-1/KDR), FGF-R1, and PDGF-R β tyrosine kinases*. *J. Med. Chem.* **2000**, *43*, 2655–2663. (d) Fong, T. A. T.; Shawver, L. K.; Sun, L.; Tang, C.; App, H.; Powell, T. J.; Kim, Y. H.; Schreck, R.; Wang, X.; Risau, W.; Ullrich, A.; Hirth, K. P.; McMahon, G. *SU5416 is a potent and selective inhibitor of the vascular endothelial growth factor receptor (Flk-1/KDR) that inhibits tyrosine kinase catalysis, tumor vascularization, and growth of multiple tumor types*. *Cancer Res.* **1999**, *59*, 99–106. (e) Laird, A. D.; Vajkoczy, P.; Shawver, L. K.; Thurnher, A.; Liang, C.; Mohammadi, M.; Schlessinger, J.; Ullrich, A.; Hubbard, S. R.; Blake, R. A.; Fong, T. A. T.; Strawn, L. M.; Sun, L.; Tang, C.; Hawtin, R.; Tang, F.; Shenoy, N.; Hirth, K. P.; McMahon, G.; Cherrington, J. M. *SU6668 is a potent antiangiogenic and antitumor agent that induces regression of established tumors*. *Cancer Res.* **2000**, *60*, 4152–4160. (f) Mendel, D. B.; Laird, A. D.; Xin, X.; Louie, S. G.; Christensen, J. G.; Li, G.; Schreck, R. E.; Abrams, T. J.; Ngai, T. J.; Lee, L. B.; Murray, L. J.; Carver, J.; Chan, E.; Moss, K. G.; Haznedar, J. O.; Sukbuntherng, J.; Blake, R. A.; Sun, L.; Tang, C.; Miller, T.; Shirazian, S.; McMahon, G.; Cherrington, J. M. *In vivo antitumor activity of SU11248, a novel tyrosine kinase inhibitor targeting vascular endothelial growth factor and platelet-derived growth factor receptors: Determination of a pharmacokinetic/pharmacodynamic relationship*. *Clin. Cancer Res.* **2003**, *9*, 327–337.
- (14) (a) Hennequin, L. F.; Stokes, E. S. E.; Thomas, A. P.; Johnstone, C.; Plé, P. A.; Ogilvie, D. J.; Dukes, M.; Wedge, S. R.; Kendrew, J.; Curwen, J. O. *Novel 4-anilinoquinazolines with C-7 basic side chains: Design and structure activity relationship of a series of potent, orally active, VEGF receptor tyrosine kinase inhibitors*. *J. Med. Chem.* **2002**, *45*, 1300–1312. (b) McCarty, M. F.; Wey, J.; Stoeltzing, O.; Liu, W.; Fan, F.; Bucana, C.; Mansfield, P. F.; Ryan, A. J.; Ellis, L. M. *ZD6474, a vascular endothelial growth factor receptor tyrosine kinase inhibitor with additional activity against epidermal growth factor receptor tyrosine kinase, inhibits orthotopic growth and angiogenesis of gastric cancer*. *Mol. Cancer Ther.* **2004**, *3*, 1041–1048. (c) Hennequin, L. F.; Thomas, A. P.; Johnstone, C.; Stokes, E. S. E.; Plé, P. A.; Lohmann, J.-J. M.; Ogilvie, D. J.; Dukes, M.; Wedge, S. R.; Curwen, J. O.; Kendrew, J.; Lambert-van der Brempt, C. *Design and structure-activity relationship of a new class of potent VEGF receptor tyrosine kinase inhibitors*. *J. Med. Chem.* **1999**, *42*, 5369–5389.
- (15) (a) Beebe, J. S.; Jani, J. P.; Knauth, E.; Goodwin, P.; Higdon, C.; Rossi, A. M.; Emerson, E.; Finkelstein, M.; Floyd, E.; Harriman, S.; Atherton, J.; Hillerman, S.; Soderstrom, C.; Kou, K.; Gant, T.; Noe, M. C.; Foster, B.; Rastinejad, F.; Marx, M. A.; Schaeffer, T.; Whalen, P. M.; Roberts, W. G. *Pharmacological characterization of CP-547,632, a novel vascular endothelial growth factor receptor-2 tyrosine kinase inhibitor for cancer therapy*. *Cancer Res.* **2003**, *63*, 7301–7309. (b) Munchhof, M. J.; Beebe, J. S.; Casavant, J. M.; Cooper, B. A.; Doty, J. L.; Higdon, R. C.; Hillerman, S. M.; Soderstrom, C. I.; Knauth, E. A.; Marx, M. A.; Rossi, A. M. K.; Sobolov, S. B.; Sun, J. *Design and SAR of thienopyrimidine and thienopyridine inhibitors of VEGFR-2 kinase activity*. *Bioorg. Med. Chem. Lett.* **2004**, *14*, 21–24.
- (16) (a) Gingrich, D. E.; Reddy, D. R.; Iqbal, M. A.; Singh, J.; Aimone, L. D.; Angeles, T. S.; Albom, M.; Yang, S.; Ator, M. A.; Meyer, S. L.; Robinson, C.; Ruggeri, B. A.; Dionne, C. A.; Vaught, J. L.; Mallamo, J. P.; Hudkins, R. L. *A new class of potent vascular endothelial growth factor receptor tyrosine kinase inhibitors: Structure-activity relationships for a series of 9-alkoxymethyl-12-(3-hydroxypropyl)indeno[2,1-a]pyrrolo[3,4-c]carbazole-5-*

- ones and the identification of CEP-5214 and its dimethylglycine ester prodrug clinical candidate CEP-7055. *J. Med. Chem.* **2003**, *46*, 5375–5388. (b) Ruggeri, B.; Singh, J.; Gingrich, D.; Angeles, T.; Albom, M.; Chang, H.; Robinson, C.; Hunter, K.; Dobrzanski, P.; Jones-Bolin, S.; Aimone, L.; Klein-Szanto, A.; Herbert, J.-M.; Bono, F.; Schaeffer, P.; Casellas, P.; Bourie, B.; Pili, R.; Isaacs, J.; Ator, M.; Hudkins, R.; Vaught, J.; Mallamo, J.; Dionne C. CEP-7055: A novel, orally active pan inhibitor of vascular endothelial growth factor receptor tyrosine kinases with potent antiangiogenic activity and antitumor efficacy in preclinical models. *Cancer Res.* **2003**, *63*, 5978–5991.
- (17) (a) Bilodeau, M. T.; Balitza, A. E.; Koester, T. J.; Manley, P. J.; Rodman, L. D.; Buser-Doepner, C.; Coll, K. E.; Fernandes, C.; Gibbs, J. B.; Heimbrook, D. C.; Huckle, W. R.; Kohl, N.; Lynch, J. J.; Mao, X.; McFall, R. C.; McLoughlin, D.; Miller-Stein, C. M.; Rickert, K. W.; Sepp-Lorenzino, L.; Shipman, J. M.; Subramanian, R.; Thomas, K. A.; Wong, B. K.; Yu, S.; Hartman, G. D. Potent *N*-(1,3-thiazol-2-yl)pyridin-2-amine vascular endothelial growth factor receptor tyrosine kinase inhibitors with excellent pharmacokinetics and low affinity for the hERG ion channel. *J. Med. Chem.* **2004**, *47*, 6363–6372. (b) Bilodeau, M. T.; Rodman, L. D.; McGaughey, G. B.; Coll, K. E.; Koester, T. J.; Hoffman, W. F.; Hungate, R. W.; Kendall, R. L.; McFall, R. C.; Rickert, K. W.; Rutledge, R. Z.; Thomas, K. A. The discovery of *N*-(1,3-thiazol-2-yl)pyridine-2-amine as potent inhibitors of KDR kinase. *Bioorg. Med. Chem. Lett.* **2004**, *14*, 2941–2945. (c) Fraley, M. E.; Arrington, K. L.; Buser, C. A.; Ciecko, P. A.; Coll, K. E.; Fernandes, C.; Hartman, G. D.; Hoffman, W. F.; Lynch, J. J.; McFall, R. C.; Rickert, K.; Singh, R.; Smith, S.; Thomas, K. A.; Wong, B. K. Optimization of the indolyl quinolinone class of KDR (VEGFR-2) kinase inhibitors: Effects of 5-amido- and 5-sulphamido-indolyl groups on pharmacokinetics and hERG binding. *Bioorg. Med. Chem. Lett.* **2004**, *14*, 351–355. (d) Fraley, M. E.; Arrington, K. L.; Hambaugh, S. R.; Hoffman, W. F.; Cunningham, A. M.; Young, M. B.; Hungate, R. W.; Tebben, A. J.; Rutledge, R. Z.; Kendall, R. L.; Huckle, W. R.; McFall, R. C.; Coll, K. E.; Thomas, K. A. Discovery and evaluation of 3-(5-thien-3-ylpyridin-3-yl)-1*H*-indoles as a novel class of KDR kinase inhibitors. *Bioorg. Med. Chem. Lett.* **2003**, *13*, 2973–2976. (e) Wu, Z.; Fraley, M. E.; Bilodeau, M. T.; Kaufman, M. L.; Tasber, E. S.; Balitza, A. E.; Hartman, G. D.; Coll, K. E.; Rickert, K.; Shipman, J.; Shi, B.; Sepp-Lorenzino, L.; Thomas, K. A. Design and synthesis of 3,7-diarylimidazopyridines as inhibitors of the VEGF-receptor KDR. *Bioorg. Med. Chem. Lett.* **2004**, *14*, 909–912. (f) Bilodeau, M. T.; Cunningham, A. M.; Koester, T. J.; Ciecko, P. A.; Coll, K. E.; Huckle, W. R.; Hungate, R. W.; Kendall, R. L.; McFall, R. C.; Mao, X.; Rutledge, R. Z.; Thomas, K. A. Design and synthesis of 1,5-diarylbenzimidazoles as inhibitors of VEGF-receptor KDR. *Bioorg. Med. Chem. Lett.* **2003**, *13*, 2485–2488. (g) Manley, P. J.; Balitza, A. E.; Bilodeau, M. T.; Coll, K. E.; Hartman, G. D.; McFall, R. C.; Rickert, K. W.; Rodman, L. D.; Thomas, K. A. 2,4-Disubstituted pyrimidines: A novel class of KDR kinase inhibitors. *Bioorg. Med. Chem. Lett.* **2003**, *13*, 1673–1677. (h) Fraley, M. E.; Rubino, R. S.; Hoffman, W. F.; Hambaugh, S. R.; Arrington, K. L.; Hungate, R. W.; Bilodeau, M. T.; Tebben, A. J.; Rutledge, R. Z.; Kendall, R. L.; McFall, R. C.; Huckle, W. R.; Coll, K. E.; Thomas, K. A. Optimization of a pyrazolo[1,5-*a*]pyrimidine class of KDR kinase inhibitors: Improvements in physical properties enhance cellular activity and pharmacokinetics. *Bioorg. Med. Chem. Lett.* **2002**, *12*, 3537–3541. (i) Fraley, M. E.; Hoffman, W. F.; Rubino, R. S.; Hungate, R. W.; Tebben, A. J.; Rutledge, R. Z.; McFall, R. C.; Huckle, W. R.; Kendall, R. L.; Coll, K. E.; Thomas, K. A. Synthesis and initial SAR studies of 3,6-disubstituted pyrazolo[1,5-*a*]pyrimidines: A new class of KDR kinase inhibitors. *Bioorg. Med. Chem. Lett.* **2002**, *12*, 2767–2770.
- (18) (a) Baidur, N.; Chadha, N.; Brandt, B. M.; Asgari, D.; Patch, R. J.; Schalk-HiHi, C.; Carver, T. E.; Petrounia, I. P.; Baumann, C. A.; Ott, H.; Manthey, C.; Springer, B. A.; Player, M. R. 2-Hydroxy-4,6-diamino-[1,3,5]triazines: A novel class of VEGFR-2 (KDR) tyrosine kinase inhibitors. *J. Med. Chem.* **2005**, *48*, 1717–1720. (b) Kuo, G.-H.; Wang, A.; Emanuel, S.; DeAngelis, A.; Zhang, R.; Connolly, P. J.; Murray, W. V.; Gruninger, R. H.; Sechler, J.; Fuentes-Pesquera, A.; Johnson, D.; Middleton, S. A.; Jolliffe, L.; Chen, X. Synthesis and discovery of pyrazine-pyridine biheteroaryl as a novel series of potent vascular endothelial growth factor receptor-2 inhibitors. *J. Med. Chem.* **2005**, *48*, 1886–1900.
- (19) Cross, M. J.; Claesson-Welsh, L. FGF and VEGF function in angiogenesis: Signalling pathways, biological responses and therapeutic inhibition. *Trends Pharm. Sci.* **2001**, *22*, 201–207.
- (20) Gerwins, P.; Skoldenberg, E.; Claesson-Welsh, L. Function of fibroblast growth factors and vascular endothelial growth factors and their receptors in angiogenesis. *Crit. Rev. Onc. Hemat.* **2000**, *34*, 185–194.
- (21) Manetti, F.; Botta, M. Small-molecule inhibitors of fibroblast growth factor receptor (FGFR) tyrosine kinases (TK). *Curr. Pharm. Des.* **2003**, *9*, 567–581.
- (22) Boehm, T.; Folkman, J.; Browder, T.; O'Reilly, M. S. Antiangiogenic therapy of experimental cancer does not induce acquired drug resistance. *Nature* **1997**, *390*, 404–409.
- (23) (a) Hunt, J. T.; Mitt, T.; Borzilleri, R.; Gullo-Brown, J.; Fargnoli, J.; Fink, B.; Han, W.-C.; Mortillo, S.; Vite, G.; Wautlet, B.; Wong, T.; Zheng, X.; Bhide, R. Discovery of the pyrrolo[2,1-*f*][1,2,4]-triazine nucleus as a new kinase inhibitor template. *J. Med. Chem.* **2004**, *47*, 4054–4059.
- (24) (a) Borzilleri, R. M.; Fargnoli, J.; Fura, A.; Gerhardt, T.; Hunt, J. T.; Mortillo, S.; Qian, L.; Tokarski, J.; Vyas, V.; Wautlet, B.; Zheng, P.; Bhide, R. S. Synthesis and SAR of 4-(3-hydroxyphenylamino)pyrrolo[2,1-*f*][1,2,4]triazine based VEGFR-2 kinase inhibitors. *Bioorg. Med. Chem. Lett.* **2005**, *15*, 1429–1433. (b) Leftheris, K.; Ahmed, G.; Chan, R.; Dyckman, A. J.; Hussain, Z.; Ho, K.; Hynes, J., Jr.; Letourneau, J.; Li, W.; Lin, S.; Metzger, A.; Moriarty, K. J.; Rivello, C.; Shimshock, Y.; Wen, J.; Wityak, J.; Wroblewski, S. T.; Wu, H.; Wu, J.; Desai, M.; Gillooly, K. M.; Lin, T. H.; Loo, D.; McIntyre, K. W.; Pitt, S.; Shen, D. R.; Shuster, D. J.; Zhang, R.; Diller, D.; Doweiko, A.; Sack, J.; Baldwin, J.; Barrish, J.; Dodd, J.; Henderson, I.; Kanner, S.; Schieven, G. L.; Webb, M. The Discovery of Orally Active Triaminotriazine Aniline Amides as Inhibitors of p38 MAP Kinase. *J. Med. Chem.* **2004**, *47*, 6283–6291.
- (25) Patil, S. A.; Otter, B. A.; Klein, R. S. Synthesis of pyrrolo[2,1-*f*][1,2,4]triazine congeners of nucleic acid purines via the *N*-amination of 2-substituted pyrroles. *J. Heterocycl. Chem.* **1994**, *31*, 781–786.
- (26) Suzuki, M.; Miyoshi, M.; Matsumoto, K. A convenient synthesis of 3-substituted pyrrole-2,4-dicarboxylic acid esters. *J. Org. Chem.* **1974**, *39*, 1980.
- (27) Belley, M.; Scheigetz, J.; Dube, P.; Dolman, S. Synthesis of *N*-aminoindole ureas from ethyl 1-amino-6-(trifluoromethyl)-1*H*-indole-3-carboxylate. *Synlett* **2001**, *2*, 222–225.
- (28) Gangloff, A. R.; Litvak, J.; Shelton, E. J.; Sperandio, D.; Wang, V. R.; Rice, K. D. Synthesis of 3,5-disubstituted 1,2,4-oxadiazoles using tetrabutylammonium fluoride as a mild and efficient catalyst. *Tetrahedron Lett.* **2001**, *42*, 1441–1443.
- (29) Diana, G. D.; Volkots, D. L.; Nitz, T. J.; Bailey, T. R.; Long, M. A.; Vescio, N.; Aldous, S.; Pevear, D. C.; Dutko, F. J. Oxadiazoles as ester bioisosteric replacements in compounds related to disoxaril. Antirhinovirus activity. *J. Med. Chem.* **1994**, *37*, 2421–2436.
- (30) Saunders, J.; Cassidy, M.; Freedman, S. B.; Harley, E. A.; Iversen, L. L.; Kneen, C.; MacLeod, A. M.; Merchant, K. J.; Snow, R. J.; Baker, R. Novel quinuclidine-based ligands for the muscarinic cholinergic receptor. *J. Med. Chem.* **1990**, *33*, 1128–1138.
- (31) Francis, J. E.; Gorczyca, L. A.; Mazzenga, G. C.; Meckler, H. A convenient synthesis of 3,5-disubstituted-1,2,4-triazoles. *Tetrahedron Lett.* **1987**, *28*, 5133–5136.
- (32) Kuo, S.-C.; Wu, C.-H.; Huang, L.-J.; Yamamoto, K.; Yoshina, S. Synthesis and antimicrobial activity of methyl 5-nitro-3,4-diphenylfuran-2-carboxylate and related compounds. *Chem. Pharm. Bull.* **1981**, *29*, 635–645.
- (33) Hervens, F.; Viehe, H. G. Heterocycles from compounds containing two nucleophilic centers and phosgene/ammonium salts. *Angew. Chem., Int. Ed. Engl.* **1973**, *12*, 405–406.
- (34) Chen, P.; Doweiko, A. M.; Norris, D.; Gu, H. H.; Spengel, S. H.; Das, J.; Moquin, R. V.; Lin, J.; Wityak, J.; Iwanowicz, E. J.; McIntyre, K. W.; Shuster, D. J.; Behnia, K.; Chong, S.; de Fex, H.; Pang, S.; Pitt, S.; Shen, D. R.; Thrall, S.; Stanley, P.; Kocy, O. R.; Witmer, M. R.; Kanner, S. B.; Schieven, G. L.; Barrish, J. C. Imidazoquinoline Src-family kinase p56^{lck} inhibitors: SAR, QSAR, and the discovery of (S)-*N*-(2-chloro-6-methylphenyl)-2-(3-methyl-1-piperazinyl)imidazo[1,5-*a*]pyrido[3,2-*e*]pyrazin-6-amine (BMS-279700) as a potent and orally active inhibitor with excellent in vivo antiinflammatory activity. *J. Med. Chem.* **2004**, *47*, 4517–4529.
- (35) Kim, K. S.; Kimball, S. D.; Misra, R. N.; Rawlins, D. B.; Hunt, J. T.; Xiao, H.-Y.; Lu, S.; Qian, L.; Han, W.-C.; Shan, W.; Mitt, T.; Cai, Z.-W.; Poss, M. A.; Zhu, H.; Sack, J. S.; Tokarski, J. S.; Chang, C. Y.; Pavletich, N.; Kamath, A.; Humphreys, W. G.; Marathe, P.; Bursucker, I.; Kellar, O. K. A.; Roongta, U.; Batorsky, R.; Mulheron, J. G.; Bol, D.; Fairchild, C. R.; Lee, F. Y.; Webster, K. R. Discovery of aminotriazole inhibitors of cyclin-dependent kinase 2: Synthesis, X-ray crystallographic analysis, and biological activities. *J. Med. Chem.* **2002**, *45*, 3905–3927.
- (36) The drug concentrations obtained during a mouse coarse oral PK study using a single 50 mg/kg dose of compound **13** were 1.8 μ M at 1 h and 0.23 μ M at 4 h.
- (37) McTigue, M. A.; Wickersham, J. A.; Pinko, C.; Showalter, R. E.; Parast, C. V.; Tempczyk-Russell, A.; Gehring, M. R.; Mroczkowski, B.; Kan, C.-C.; Villafraña, J. E.; Appel, K. Crystal

- structure of the kinase domain of human vascular endothelial growth factor receptor 2: A key enzyme in angiogenesis. *Structure* **1999**, *7*, 319–330.
- (38) Version 3.5, Schrodinger, LLC: New York, 2005.
- (39) Hagler, A. T.; Ewig, C. S. On the use of quantum energy surfaces in the derivation of molecular force fields. *Comput. Phys. Comm.* **1994**, *84*, 131–155.
- (40) Kuramoto, Y.; Ohshita, Y.; Yoshida, J.; Yazaki, A.; Shiro, M.; Koike, T. A novel antibacterial 8-chloroquinolone with a distorted orientation of the *N*1-(5-amino-2,4-difluorophenyl) group. *J. Med. Chem.* **2003**, *46*, 1905–1917.
- (41) Armarego, W. L. F.; Taguchi, H.; Cotton, R. G. H.; Battiston, S.; Leong, L. Lipophilic 5,6,7,8-tetrahydropterin substrates for phenylalanine hydroxylase (monkey brain), tryptophan hydroxylase (rat brain), and tyrosine hydroxylase (rat brain). *Eur. J. Med. Chem.* **1987**, *22*, 283–291.
- (42) Francisco, J. A.; Gawlak, S. L.; Siegall, C. B. Construction, expression, and characterization of BD1-G28-5 sFv, a single-chain anti-CD40 immunotoxin containing the ribosome-inactivating protein bryodin I. *J. Biol. Chem.* **1997**, *272*, 24165–24169.

JM0501275